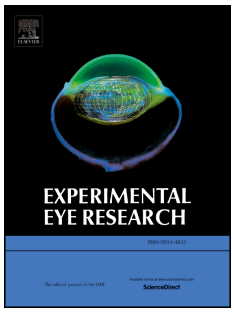

Natural immunoglobulin M-based delivery of a complement alternative pathway inhibitor in mouse models of retinal degeneration

Balasubramaniam Annamalai, Nathaniel Parsons, Crystal Nicholson, Kusumam Joseph, Beth Coughlin, Xiaofeng Yang, Bryan W. Jones, Stephen Tomlinson, Bärbel Rohrer

PII: S0014-4835(21)00148-2

DOI: https://doi.org/10.1016/j.exer.2021.108583

Reference: YEXER 108583

To appear in: *Experimental Eye Research*

Received Date: 13 July 2020

Revised Date: 31 March 2021

Accepted Date: 13 April 2021

Please cite this article as: Annamalai, B., Parsons, N., Nicholson, C., Joseph, K., Coughlin, B., Yang, X., Jones, B.W., Tomlinson, S., Rohrer, Bä., Natural immunoglobulin M-based delivery of a complement alternative pathway inhibitor in mouse models of retinal degeneration, *Experimental Eye Research* (2021), doi: https://doi.org/10.1016/j.exer.2021.108583.

Natural immunoglobulin M-based delivery of a complement alternative pathway inhibitor in mouse models of retinal degeneration.

Balasubramaniam Annamalai[1], Nathaniel Parsons[1], Crystal Nicholson[1], Kusumam Joseph[1], Beth Coughlin[1], Xiaofeng Yang[2], Bryan W. Jones[3], Stephen Tomlinson[2, 4], Bärbel Rohrer[1, 4, 5#]

Departments of Ophthalmology[1], Microbiology and Immunology[2] and Neurosciences[5]; and Medical University of South Carolina, Charleston, SC, USA; [3]Department of Ophthalmology, University of Utah, Salt Lake City, UT, USA. [4]Ralph H. Johnson VA Medical Center, Division of Research, Charleston, SC, USA.

#Addresses for correspondence

BR: Department of Ophthalmology, Medical University of South Carolina, 167 Ashley Avenue, Charleston, SC 29425; phone: (843) 792-5086; fax (843) 792-1723; e-mail: rohrer@musc.edu.

Figures: 8 Tables: 0

Abstract word count: 244

Manuscript total word count (excl. abstracts, acknowledgements, references and figure legends): 7191

Keywords: complement system; choroidal neovascularization; smoke-induced ocular pathology; natural antibody-mediated targeting; alternative pathway inhibitor; encapsulated ARPE-19 cells.

ABSTRACT

Purpose: Age-related macular degeneration is a slowly progressing disease. Studies have tied disease risk to an overactive complement system. We have previously demonstrated that pathology in two mouse models, the choroidal neovascularization (CNV) model and the smoke-induced ocular pathology (SIOP) model, can be reduced by specifically inhibiting the alternative complement pathway (AP). Here we report on the development of a novel injury-site targeted inhibitor of the alternative pathway, and its characterization in models of retinal degeneration.

Methods:

Expression of the danger associated molecular pattern, a modified annexin IV, in injured ARPE-19 cells was confirmed by immunohistochemistry and complementation assays using B4 IgM mAb. Subsequently, a construct was prepared consisting of B4 single chain antibody (scFv) linked to a fragment of the alternative pathway inhibitor, fH (B4-scFv-fH). ARPE-19 cells stably expressing B4-scFv-fH were microencapsulated and administered intravitreally or subcutaneously into C57BL/6J mice, followed by CNV induction or smoke exposure. Progression of CNV was analyzed using optical coherence tomography, and SIOP using structure-function analyses. B4-scFv-fH targeting and AP specificity was assessed by Western blot and binding experiments.

Results: B4-scFv-fH was secreted from encapsulated RPE and inhibited complement in RPE monolayers. B4-scFv-fH capsules reduced CNV and SIOP, and western blotting for C3a, C3d, IgM and IgG confirmed a reduction in complement activation and antibody binding in RPE/choroid.

Conclusions: Data supports a role for natural antibodies and neoepitope expression in ocular disease, and describes a novel strategy to target AP-specific complement inhibition to diseased tissue in the eye.

Precis: AMD risk is tied to an overactive complement system, and ocular injury is reduced by alternative pathway (AP) inhibition in experimental models. We developed a novel inhibitor of the AP that targets an injury-specific danger associated molecular pattern, and characterized it in disease models.

INTRODUCTION

Age-related macular degeneration (AMD) is a slowly progressing neurodegenerative disease (Sieving, 2005) that occurs in two forms: wet and dry, with the dry form making up 80-90% of total cases (Brown et al., 2005). RPE/choroid interface disturbances are common to both forms of the disease, and include thickening of Bruch's membrane, which includes sub-RPE deposits and drusen formation, and deterioration of the blood retina barrier. The main pathological difference between dry and wet AMD is that dry AMD RPE pathology leads to the slow degeneration and atrophy of the photoreceptors in the macula by mechanisms not fully understood, whereas in wet AMD, damage is caused by fluid leakage from choroidal neovascularization (CNV) in the macula.

The complement system is an essential part of the innate and adaptive immune system, and it is now accepted that an overactive complement system is tied to the incidence of AMD, based on histological, biochemical and genetic data (Scholl et al., 2008). Complement has important roles in many homoeostatic mechanisms (Fearon, 1998; Holers, 2000), but inappropriate or excessive complement activation is involved in the pathogenesis of autoimmune, inflammatory and ischemic diseases (Holers, 2003). Complement is activated by three pathways: classical (CP), lectin (LP) and alternative pathway (AP) (Muller-Eberhard, 1988). Importantly, while CP/LP activation is specific, requiring an initial interaction with specific ligands, including IgG or IgM bound to their respective ligands on surfaces, AP activation can occur spontaneously or as part of the AP amplification loop. All activation pathways lead to the formation of biological effector molecules, including the anaphylatoxins C3a and C5a which recruit and activate immune cells, opsonins C3b, iC3b, C3dg and C3d, which become covalently bound to activating surfaces and act as ligands for receptors on immune cells, and the cytolytic membrane attack complex (MAC).

Evidence indicates that the AP is the most potent driver of AMD in both patients and animal models.(Clark and Bishop, 2018; Tan et al., 2016).

It is of interest that recent studies have suggested that autoantibodies (aAbs) and hence the corresponding ligands play a role in AMD pathogenesis. AMD patients, both early- and late-stage, have elevated levels of IgG aAbs when compared to controls (Patel et al., 2005), with reactivities that include GFAP (Joachim et al., 2007), carboxyethylpyrrole (CEP) (Gu et al., 2003), □-crystallin, □-enolase (Joachim et al., 2007), annexin II (Umeda et al., 2005), and cardiolipin (Ozkan et al., 2012). Proof of concept that aAbs are involved in disease was provided by immunizing mice with CEP-adducted BSA with the subsequent development of ocular pathology similar to dry AMD [15], and pathology in the smoke-induced ocular pathology model, which is complement dependent, was amplified by immunization with oxidized elastin peptides (Annamalai et al., 2020a; Hollyfield et al., 2010). There is a distinction between so called self-reactive natural antibodies (nAbs) and aAbs. nAbs have a germline/near germline sequence, are polyreactive with low affinity, recognize antigens without prior exposure, and are predominantly IgM. Autoantibodies are generally specific high affinity somatically mutated IgG (Elkon and Casali, 2008). While the host defense system utilizes nAbs to respond to common microbial pathogens (recognition of non-self) (Baumgarth et al., 2005), there is evidence that they also contribute to tissue homeostasis. In particular, and relevant to this report, nAbs contribute to tissue homeostasis by activating complement on apoptotic or damaged cells and thus tagging them for removal (Silverman et al., 2009). Interestingly, in naive mice, nAbs to neoepitopes or damage associated molecular patterns (DAMPs) are dominated by specificities to phosphorylcholine (PC) and malondialdehyde (MDA) (Chen et al., 2009), but also include cardiolipin, phosphatidylserine and annexin IV (e.g. (Elvington et al., 2012)). Relevant to AMD,

an antigen microarray analysis revealed a small set of nAbs that correlated with dry or wet AMD diagnoses (Morohoshi et al., 2012). Finally, in oxidatively stressed RPE cells we have shown that a natural antibody termed C2-IgM detects MDA and PC epitopes and triggers complement activation via the LP pathway. Furthermore, in a mouse model, C2-IgM augmented CNV development in rag1$^{-/-}$ mice (Joseph et al., 2013).

We previously developed an AP complement inhibitor molecule that enables specific tissue targeting. This inhibitor termed CR2-fH was efficacious in both *in vitro* (Joseph et al., 2013; Thurman et al., 2009) and *in vivo* models of AMD (Rohrer et al., 2009; Woodell et al., 2016). CR2-fH consists of the N-terminus of mouse complement factor H (short consensus repeats [SCR] 1-5), which contains the AP-inhibitory domain, linked to a complement receptor 2 (CR2) fragment that binds complement C3 activation products (Holers et al., 2013). Hence, the CR2 domain targets the inhibitor fH to sites of complement activation, where it locally inhibits AP activation (Rohrer et al., 2009). *In vivo*, we have shown that when injected intravenously, CR2-fH reduces CNV development by reducing complement activation and VEGF production (Rohrer et al., 2012; Rohrer et al., 2009). CR2-fH also promoted the regression of deposits in BrM generated in response to long-term smoke inhalation (smoke induced ocular pathology, SIOP) in mice (Woodell et al., 2016). Finally, we have demonstrated efficacy of administration of encapsulated ARPE-19 cells producing CR2-fH inhibitor in the mouse CNV and the SIOP model (Annamalai et al., 2018; Annamalai et al., 2020b). In a separate animal model, we have demonstrated that in addition to complement C3 activation products, DAMPs can also be used for therapeutic targeting. Specifically, a specific self-reactive pathogenic IgM (termed B4) has been investigated. B4 was identified from hybridomas created from B cells of unmanipulated C57BL/6 mice and was demonstrated to recognize mouse annexin IV (Kulik et al., 2009). A

single-chain variable fragment of B4 (B4-scFv) has been shown to bind directly to recombinant annexin IV, to competitively inhibit the binding of B4 mAb to annexin IV, and when linked to a complement inhibitor to reduce complement activation in a dose-dependent manner in a zymozan assay (Atkinson et al., 2015) and to inhibit complement activation and injury in animal models (Alawieh et al., 2018; Atkinson et al., 2015).

Here we combine three therapeutic approaches for AMD; first, fH as an AP inhibitor to reduce complement activation. Second, a targeting domain for fH, which is a previously characterized natural antibody recognizing the DAMP annexin IV on oxidatively stressed surfaces (B4) (Elvington et al., 2012). And third, the use of encapsulated cells for the long-term production of the therapeutic in vivo (Annamalai et al., 2018). Together, we will investigate the efficacy of B4-scFv-fH delivery via cell-encapsulation of genetically modified ARPE-19 cells in mouse models of AMD.

METHODS

Cell culture.

ARPE-19 cells (ATCC® CRL-2302™; American Type Culture Collection, Manassas, VA) were expanded in Dulbecco's modified Eagle's medium F12 (Invitrogen) with 10% fetal bovine serum (FBS) and antibiotics as described before (Thurman et al., 2009).

IgMs used in vitro and in vivo

The B4 IgM mAb derived from hybridomas was previously described (Kulik et al., 2009) and found to be specific for post-translationally modified annexin IV. Two IgM antibodies were used as isotype controls; F632 and F1102 IgM mAb and gave identical (negative) results in all experiments used (data not shown), and will be referred to as control IgM antibody. F632 IgM was raised against 4-hydroxy-3-nitrophenylacetyl (NP)-KLH, F1102 IgM against dinitrophenol, and were described previously (Atkinson et al., 2015; Joseph et al., 2013). Purification of B4 and control IgMs was performed as described previously (Elvington et al., 2012).

Transepithelial resistance (TER) measurements.

ARPE-19 cells were grown as mature monolayers on 6-well Transwell inserts (0.4 μm PET, 24 mm insert; Corning, Corning, NY) as previously described (Ablonczy and Crosson, 2007). After 5-6 weeks, and 2-3 days prior to experiments, cells were changed to serum-free media. Complement was activated using 0.5 mM H_2O_2 and 10% normal human serum (NHS; pooled NHS from Quidel Corporation, Santa Clara, CA) as reported previously (Thurman et al., 2009). Complement attack results in sublytic complement activation, leading to VEGF release and a concomitant reduction in barrier function (Thurman et al., 2009), making TER measurements a convenient readout for the level of complement activation (Joseph et al., 2013). TER was determined by measuring the resistance across the monolayer with an EVOM volt-ohmmeter (World Precision Instruments, Sarasota, FL).(Thurman et al., 2009) To analyze the involvement of immunoglobulins (Ig) in triggering complement activation, Ig-depleted serum was obtained from Sunnylab (Sittingbourne, UK); and reconstitution experiments were performed by adding back antigen-specific (B4 IgM) or control IgMs (see previous section).

Immunofluorescence staining.

Surface exposure of IgM-specific epitopes was examined by immunofluorescence microscopy as published previously (Joseph et al., 2013). To trigger DAMP expression, ARPE-19 cells were grown on 35-mm lysine-coated glass-bottom culture dishes (MatTek Corporation; Ashland, MA) and treated with 0.5 mM H_2O_2 or 10% smoke extract for 10 minutes. Expression of B4 DAMP was determined using IgM B4 mAb (1:100 IgM B4) followed by FITC-labeled goat anti-mouse IgM (1:200; Zymed Laboratories; Invitrogen, Carlsbad, CA). Alternatively, cells were exposed to 150 □g/mL B4-scFv-fH, followed by FITC-labeled mouse anti-His IgG (1:200; Abcam, Cambridge, MA). As a negative control, primary antibody or B4-scFv-fH were omitted. Staining was also performed on CNV lesions (see below for induction of CNV) as reported previously (Joseph et al., 2013), incubating eyecups with IgM B4 mAb (1:200), followed by anti-mouse IgM (1:200). Omission of primary antibody served as the negative control. Staining of cells and flatmounts was examined by confocal microscopy (Olympus FluoView, Olympus, Center Valley, PA).

Stably transfected ARPE-19 cells expressing B4scFv-fH.

The B4-scFv expression plasmid (PBM vector) was constructed from sequences isolated from the corresponding B4 hybridoma as described (Atkinson et al., 2015). For construction of the B4-scFv-fH expression plasmid, the B4-scFv sequence was linked to the 5 N-terminal SCRs of mouse fH (residues 1-303 of mature protein, RefSeq NM009888) by overlapping PCR with the linker (G4S2)2, and OKT3 light chain signal peptide sequence added to the 5′ end of the VH

chain. A His tag encoding sequence was added to the C terminus of the fH sequence. Recombinant protein was expressed in CHO cells and purified by anti-His tag affinity chromatography as described (Atkinson et al., 2005).

ARPE-19 cells (ATCC® CRL-2302™; American Type Culture Collection, Manassas, VA), a human RPE cell line was used for encapsulation as described previously (Annamalai et al., 2018; Belhaj et al., 2020). These cells were grown in DMEM-F12 (Gibco, Thermo Fisher, Waltham, MA) with 10% fetal bovine serum (FBS) and 1 x Penicillin/streptomycin. The B4-scFv-fH plasmid construct was transfected into ARPE-19 cells with FuGene HD transfection reagent according to the manufacturer's instructions (Roche Applied Science, Indianapolis, IN), and stable expression of a mixed population of drug resistant cells was generated using kanamycin selection. B4-scFv-fH secretion into the apical and basal compartment was monitored in polarized RPE grown on transwell plates (**Fig. 4**) (Thurman et al., 2009).

Dot Blot and Western Analysis

To determine whether stably transfected cells produce detectable B4-scFv-fH, apical and basal supernatants were collected and probed as reported previously (Annamalai et al., 2018), using an antibody against the His tag (1:1000; TaKaRa, Mountain View CA). To determine complement activation and antibody deposition in the eye, RPE/choroid samples were collected, protein extracted, separated by electrophoresis and transferred to a PVDF membrane, and membranes incubated with primary antibody against C3d (clone 11) (Thurman et al., 2013), IgG or IgM as published previously (Annamalai et al., 2020a) and corresponding C3□ fragments identified according to molecular weight (Thurman et al., 2013). To determine a potential immune

response, supernatant from B4-scFv-fH-expressing cultured ARPE-19 cells were separated by electrophoresis, and membranes probed with the primary antibody against His, or serum (1:50) from mice treated with B4-scFv-fH or empty capsules. Proteins were visualized with horseradish peroxidase-conjugated secondary antibodies (Santa Cruz Biotechnology, Dallas TX) followed by incubation with Clarity™ Western ECL Blotting Substrate and chemiluminescent detection.

C3a Elisa

The C3a Elisa was carried out according to the manufacturer instructions using the mouse complement C3 Elisa from LifeSpan Biosciences, Inc, and as reported previously (Annamalai et al., 2018). In short, the RPE/choroid tissues were quickly rinsed with ice cold PBS to remove excess blood. Tissues were lysed by ultrasonication using 500 □L ice cold PBS. The final homogenate was centrifuged at 5000*g* for 5 minutes and then subjected to the assay procedure as directed by the manufacturer, using 100 □L per well. Purified mouse C3a at known concentrations was used as a standard. Measurements were obtained using the microplate reader set at 450 nm.

Cell encapsulation

Cell encapsulation was performed using our published protocol (Annamalai et al., 2018) (Belhaj et al., 2020). In short, stably transfected ARPE-19 cells were suspended at $1x10^6$ cells in 300 □L alginate solution (high mannuronic acid content, low viscosity; Sigma-Aldrich, St. Louis, MO) and pumped through a needle (30G blunt tip; Small Parts, Inc., Logansport, IN) into a gelling bath (10 mM HEPES buffered saline containing 100 mM $CaCl_2$ [Sigma-Aldrich] and 0.5% w/v poly-L-ornithine [PLO; Alfa Aesar, Haverhill, MA]). To produce microcapsules with a

size of ~150 μm, the following parameters were used: flow rate of 60 mm/h and voltage of 8.0 kV. PLO in the gelling bath forms a second coating to the microcapsules using a one-step method for adjusting the porosity. Cell recovery from microcapsules and cell viability in microcapsules has already been confirmed (Annamalai et al., 2018).

Mice

C57BL/6J (B6) and B6 rag1$^{-/-}$ mice were generated from breeding pairs (Jackson Laboratory; Bar Harbor, ME). Mice entered the study at 3 months of age, and both sexes were included. All animal experiments were performed in accordance with the ARVO Statement for the Use of Animals in Ophthalmic and Vision Research and were approved by the University Animal Care and Use Committee.

Capsule Injections

Two delivery sites were used, intraocular and subcutaneous. Intravitreal injections were performed under visual inspection as previously described (Annamalai et al., 2018). In short, mice were anesthetized by intraperitoneal injection (xylazine and ketamine, 20 and 80 mg/kg respectively), eyes dilated (2.5% phenylephrine HCL and 1% atropine sulfate), and 1 □L injections administered behind the limbus using a 27 gauge needle attached to a Hamilton syringe through a preformed guide hole made with a 26 x 3/8 gauge beveled needle. Antibiotic ointment was used as a precaution. The same effective concentration established in an earlier study for a different complement inhibitor (~10 capsules/□L) was used (Annamalai et al., 2018). For subcutaneous injections, 50 capsules/100 □L microcapsules were mixed in 100 □L Matrigel (BD Biosciences, Franklin Lakes, NJ) and drawn up in an insulin syringe. Mice were

anesthetized with isoflurane and injected into the back, pinching the skin and injecting the microcapsules into the pouch (Reuter, 2011).

Laser choroidal neovascularization

One month following the intravitreal injection, argon laser photocoagulation (532 nm, 100 μm spot size, 0.1 s duration, 100 mW) was used to generate 4 laser spots around the optic nerve of each eye (Rohrer et al., 2009). As previously described, bubble formation at the site of the laser burn was used to confirm Bruch's membrane rupture, and only those lesions were assessed for lesion growth (Nozaki et al., 2006a).

Reconstitution experiments

Rag1$^{-/-}$ mice used in the CNV study were treated on days 0, 2 and 4 after the induction of laser CNV with B4 IgM or control IgM (100 □g diluted in 400 □L PBS) using intraperitoneal (IP) injections. IP injections have been shown to be effective for antibody delivery to CNV lesions in C57BL/6J mice (Campa et al., 2008), and for the reconstitution of rag1$^{-/-}$ mice with specific antibodies (Joseph et al., 2013).

Exposure to Cigarette Smoke.

One month following the subcutaneous injection, mice were subjected to cigarette smoke exposure (CSE). CSE , which was carried out for 5 hours per day, 5 days per week, by burning 3R4F reference cigarettes (University of Kentucky, Louisville, KY) using a smoking machine

(Model TE-10; Teague Enterprises, Woodland, CA) over a period of 6 months as published previously (Woodell et al., 2013).

Assessment of CNV lesion volume by confocal microscopy

Relative CNV size was determined in flat-mount preparations of RPE-choroid stained with isolectin B (which binds to terminal β-D-galactose residues on endothelial cells and selectively labels the murine vasculature) (Nozaki et al., 2006b). This methodology was described by us previously in detail (Rohrer et al., 2012; Rohrer et al., 2009). In brief, immersion-fixed (4% paraformaldehyde) eyecups were labeled with Isolectin B (1:100 of 1 mg/mL solution; Sigma-Aldrich, St. Louis, MO), flattened using relaxing cuts and examined by confocal microscopy (Leica TCS SP2 AOBS, Leica Bannockburn, IL). Z-stacks of fluorescent images (2 □m sections) through the depth of the lesions were obtained, and pixel intensity against depth was obtained, from which the area under the curve (indirect volume measurement) was calculated. Data are expressed as mean ± SEM per eye. Individual CNV lesions were also photographed using a fluorescent microscope (Zeiss, Thornwood, New York).

Assessment of CNV lesion diameters by Optical Coherence Tomography

Optical coherence tomography (OCT) was used to analyze CNV lesion size on day 5 post laser treatment using an SD-OCT Bioptigen® Spectral Domain Ophthalmic Imaging System (Bioptigen Inc., Durham NC) as previously described (Coughlin et al., 2016; Schnabolk et al., 2015; Schnabolk et al., 2014), examining acquired rectangular volume scans (images set at 1.6 x1.6 mm, consisting of 100 B-scans, 1000 A-scans per B scan) using Image J software (Wayne

Rasband, National Institutes of Health, Bethesda, MD). The area around the hyporeflective spot produced on the fundus image was measured with vertical calipers set at 0.100 mm at the site of each lesion. (Giani et al., 2011) Diameter obtained in number of pixels (1.6 x 1.6 □m) was converted into □m^2.

Optokinetic Response Test

Visual acuity and contrast sensitivity of mice were measured under photopic conditions (mean luminance of 52 cd m^{-2}) by observing reflexive optomotor responses to moving sine-wave gratings (OptoMotry, Cerebral Mechanics, Lethbridge, AB) as previously described.(Woodell et al., 2013) In short, visual acuity was measured by finding the spatial frequency threshold of each animal at a constant speed (12 deg/s) and contrast (100%) with a staircase procedure. Contrast sensitivity was determined by taking the reciprocal of the contrast threshold at a fixed spatial frequency (0.131 cyc/deg) and speed (12 deg/s).

Electron Microscopy

Tissue preparation and ultrastructural analyses were performed as previously described (Woodell et al., 2016). Transmission electron microscopy (TEM) images were captured using a JEOL JEM 1400 transmission electron microscope (JEOL USA Inc., Peabody MA) using SerialEM software (https://bio3d.colorado.edu/SerialEM/), capturing 1200–1500 images per section, yielding datasets that were then processed with the NCR Toolset (Scientific Computing and Imaging Institute, Salt Lake City, UT) (Anderson et al., 2009; Stoppelkamp et al., 2010) to generate image mosaics. Images were evaluated using Adobe® Photoshop® (Adobe Systems,

San Jose, CA) and ImageJ software (National Institutes of Health) as published previously.(Woodell et al., 2013) For each animal, BrM thickness was determined by analyzing ~24 μm length sections of damaged BrM areas of each sample. Areas of each BrM sample were outlined measuring 1.22 □m away from the choroidal intercapillary pillars, using the basement membrane of the RPE and choriocapillaris as boundaries. BrM thickness in age-matched room air exposed mice was consistently 0.22 ± 0.04 □m, and a thickness exceeding 0.28 □m was considered damaged (Annamalai et al., 2020a).

Data Analysis and Statistics

Data are presented as mean ±SEM. Single comparisons were analyzed using unpaired t-tests. Data consisting of multiple groups were analyzed by ANOVA (Fisher PLSD), with mean value differences considered significant at $P \leq 0.05$ (StatView, SAS Institute, Inc., Cary, NC).

RESULTS

Identification of ligands for a natural IgM on RPE cells in vitro and in vivo.

Complement activation on the RPE cell surface has been shown to be involved in AMD-related pathology. Previously, we have shown that oxidative stress generated by either H_2O_2 (Thurman et al., 2009) or smoke exposure (Kunchithapautham et al., 2014) can sensitize ARPE-19 cells grown in monolayers to complement attack. In follow-up experiments aimed at identifying stress/injury related ligands on the cell surface of RPE cells, as well as the complement pathway involved leading to complement activation upon H_2O_2 exposure, we showed that the LP initiated the complement cascade which was then amplified by the AP, and further that LP activation

required natural antibody recognition of neoepitopes (Joseph et al., 2013). One of the neoepitopes generated on RPE cells upon H_2O_2 exposure is recognized by the C2 IgM mAb, an antibody previously characterized as recognizing a subset of phospholipids that included phosphatidylcholine (PC) and malondialdehyde (MDA), an end-product of lipid peroxidation (Joseph et al., 2013). A second self-reactive IgM mAb known as B4 has been shown to recognize a post-ischemic neoepitope identified as post translationally modified annexin IV in mouse cells (Elvington et al., 2012; Kulik et al., 2009). Here we further demonstrate the presence of the B4 epitope on oxidatively-stressed human RPE cells and characterize its involvement in complement activation.

Immunohistochemistry was performed to determine the reactivity of IgM B4 on oxidatively stressed ARPE-19 cell monolayers. B4 neoepitope was identified in a punctate pattern across the apical surface on H_2O_2- or smoke-treated cells, with little or no presentation of a B4 epitope expressed on control uninjured cells (**Fig. 1, top row**).

We have shown that the LP receptors ficolin/MASP or MBL/MASP require immunoglobulins, and specifically natural IgM, to initiate complement activation on the cell surface of RPE cells (Joseph et al., 2013). As a physiological readout for complement activation we have used the readout of TER. In this assay, oxidative stress generated by H_2O_2 reduces endogenous complement inhibition at the cell surface of ARPE-19 monolayers, triggering sublytic complement activation that results in secretion and mobilization of VEGF (Bandyopadhyay and Rohrer, 2012; Thurman et al., 2009), which in turn reduces TER due to its effect on tight junction stability (Ablonczy and Crosson, 2007). Using TER reduction as the readout, we had shown previously that while complement-sufficient serum reduced TER by 40-50%, Ig-depleted serum was ineffective. Importantly, C2 IgM-C2 addition to Ig-depleted serum reconstituted

activity in the TER assay (Joseph et al., 2013). Here we extended this analysis to B4 IgM mAb. First, we reconfirmed that 4 hours after the addition of H_2O_2 and complement-sufficient serum (complete NHS), TER was reduced by ~50%, whereas the addition of H_2O_2 and Ig-depleted serum had no effect (**Fig. 2A**). However, addition of B4 IgM mAb to Ig-depleted serum reconstituted activity in the TER assay to levels indistinguishable from normal human serum. The control antibody had no effect, and TER under control conditions was identical to that of Ig-depleted serum (**Fig. 2A**).

MDA-neoepitopes have been identified in mouse CNV lesions by immunohistochemistry (Weismann et al., 2011) as well as in BrM or AMD patients (Weismann et al., 2011). Also, annexins have been identified in Bruch's membrane and drusen in human patients (Rayborn et al., 2006). The functional consequence of antibody binding to MDA neoepitopes has been analyzed by us, and we showed that CNV lesions in rag1$^{-/-}$ mice can be augmented by injections of C2 IgM mAb. Rag1$^{-/-}$ mice produce no mature T-cells or B-cells and are therefore antibody-deficient. In other disease models (Elvington et al., 2012) as well as the CNV lesion model (Joseph et al., 2013), rag1$^{-/-}$ mice have been used in reconstitution experiments to demonstrate that particular self-reactive antibodies are involved in the development of disease. Here, we examined C57BL/6J mouse CNV laser lesions by immunohistochemistry for labeling with the B4 mAb. Diffuse labeling with B4 mAb was seen in CNV lesions as opposed to the area surrounding the lesion (**Fig. 3A**). When CNV lesions were examined in rag1$^{-/-}$ mice after 3 administrations of B4 mAb every 48 hours, CNV lesions were significantly increased compared to rag1$^{-/-}$ mice treated with either PBS or control IgM (P<0.01) (**Fig. 3B**). Administration of B4 mAb to wildtype mice had no effect (data not shown).

Generation of encapsulated ARPE-19 cells

ARPE-19 cells were transfected using FuGene HD, and stable expression in a mixed population was enforced by antibiotic selection as reported previously (Annamalai et al., 2018). Secretion of B4-scFv-fH from ARPE-19 monolayers was confirmed by dotblot analysis of both apical and basal supernatants collected from cells grown on transwell plates as stable monolayers (**Fig. 4A**). Following confirmation of stable secretion of scFv-fH, complement inhibitory activity was confirmed in the TER assay. Specifically, we determined that the amount of B4-scFv-fH secreted by ARPE-19 cells is sufficient to protect against the drop in TER induced by H_2O_2 and complement-sufficient serum exposure. Forty-eight hours after the previous media change, media was collected from B4-scFv-fH transfected and control cells. The undiluted media was added to naïve monolayer which were subsequently exposed to 0.5 mM H_2O_2 and 5% NHS, which reduced TER. Monolayers treated with B4-scFv-fH were significantly protected indicating that ARPE-19 cells secrete functional intact complement inhibitor at concentrations sufficient to reduce complement activation *in vitro* (**Fig. 2B**). When using purified B4-scFv-fH to identify binding sites on oxidatively stressed ARPE-19 cell monolayers, a similar staining patters as for the B4IgM mAb was identified. Again, a punctate pattern across the apical surface on H_2O_2- or smoke-treated cells was identified, with little or no binding to non-stressed cells (**Fig. 1, bottom row**).

Intravitreal delivery of encapsulated ARPE-19 cells reduces CNV

We have previously determined that the appropriate size of capsules suitable for injection through a 27 gauge needle is 150 □m, and have documented the presence of the intact capsules in the mouse vitreous after injection by OCT (Annamalai et al., 2018).

Here we evaluated the effect of encapsulated ARPE-19 cells expressing B4-scFv-fH on CNV lesion size 5 days following laser-induced photocoagulation. The same concentration of B4-scFv-fH-expressing ARPE-19 cells that was shown to be efficacious for CR2-fH (10 capsules in 1 □L media) was injected intravitreally and outcomes compared to control (empty) ARPE-19 cells. After ~1 month, CNV was induced by laser-photocoagulation of Bruch's membrane (BrM) in all four quadrants of the eye, and on day 5, CNV lesion sizes were assessed using OCT. B4-scFv-fH treatment significantly decreased (P <0.05) lesion sizes compared to control (empty capsules) treatment (**Fig. 5A, B**).

The presence of B4-scFv-fH, complement activation products and IgG/IgM in the RPE/choroid fractions was assessed by dot blot, ELISA and Western blotting. Dot blot analysis showed the presence of B4-scFv-fH in the RPE/choroid of injected animals as expected (**Fig. 6A**), with less being present in the retina. Factor H inhibits and inactivates the alternative pathway C3 convertase that generates C3b (consisting of both an □' and □ chain) and C3a, the C3□' chain (~101 kDa) is then subsequently cleaved to generate C3□'1 (63 kDa) by factor I and cofactor, followed by cleavage by factor I and CR1 to C3dg (39 kDa) and by tryptic enzymes to C3dg (34 kD) (Thurman et al., 2013). Western blot analyses to detect the proteolytic cleavage products of C3□□□using an antibody against the C3d domain (Thurman et al., 2013), demonstrated that B4-scFc-fH injected mice had significantly lower levels of C3□' (P <0.01), C3□'1 (P <0.05) and C3dg/C3d (P <0.01) in the RPE/choroid fraction (**Fig. 6B, B'**), indicative of reduced C3 activation. Please note that due to the similar molecular weights of C3dg and C3d, the two bands

could not be cleanly resolved and are reported together. As assayed by a sensitive ELISA determinations, there was a significant increase in the level of C3a in the RPE/choroid in mice with, compared to mice without, CNV (P <0.0001). C3a levels were completely normalized back to baseline by B4-scFv-fH (empty capsules versus B4-scFv-fH: P <0.0001; B4-scFv-fH versus control: P =0.19; **Fig. 6C**). The targeting of B4-scFv-fH to CNV lesions suggests that complement is activated in an IgG- and/or IgM-dependent manner (Saeed et al., 2017). The same RPE/choroid samples were probed for the presence of IgG and IgM antibodies using quantitative Western blotting (**Fig. 6D, D'**). B4-scFv-fH significantly decreased both IgG and IgM levels in the RPE/choroid fraction when compared to the empty capsules (P <0.001).

Subcutaneous delivery of encapsulated ARPE-19 cells reduces SIOP

Neoepitopes generated by smoke are recognized by B4 mAb (**Fig. 1A**), and smoke exposure in animals leads to complement-dependent pathology in the RPE (Woodell et al., 2013) that is treatable with the AP inhibitor CR2-fH (a C3d targeted inhibitor) (Woodell et al., 2016). Based on these observations, we tested the effectiveness of encapsulated ARPE-19 cells expressing B4-scFv-fH to prevent SIOP when delivered systemically. We investigated systemic capsule delivery as an alternative means of intraocular treatment for two reasons. First, long-term stability (6 months) of alginate capsules in the eye cannot be guaranteed, and accidental release of cells into the vitreous may have unwanted consequences; and second, complement activation occurs on the basal side of the RPE, as well as on BrM and the choriocapillaris, and delivery of B4-scFv-fH across the blood retina barrier is not guaranteed. In previously published experiments, the equivalent effective concentration of subcutaneously injected CR2-fH expressing capsulated cells (described in (Annamalai et al., 2018)) when compared to

intravenously delivered protein (described in (Rohrer et al., 2009)) to reduce CNV progression was determined to be ~1000 capsules (Annamalai et al., 2020b).

Encapsulated ARPE-19 cells expressing B4-scFv-fH were deposited subcutaneously in matrigel in the neck region of 2 month-old mice. After ~1 month, animals were exposed to long-term smoke inhalation as reported previously (Woodell et al., 2013). After the completion of the 6-month smoke exposure, animals were assessed for visual function using optokinetic responses, followed by tissue analysis and assessment of anti-drug antibodies.

To ensure lack of antibody development against B4-scFv-fH, we assessed whether mice generate antibodies against the fusion protein 7 months after the deposition of the capsules. No IgG or IgM antibodies recognizing B4-scFv-fH could be detected in serum from experimental animals (Fig. 4B).

As reported previously, spatial acuity in C57BL/6J mice was not affected by CSE as compared to room air exposure (data not shown). However, contrast threshold (% contrast required to elicit a response) was reduced in CSE mice treated with empty capsules, which exhibited a significant decrease in contrast sensitivity compared to never-smokers (empty capsules: 51.7 ±7.0 versus never-smokers: 8.78 ±0.43; $P<0.0001$; **Fig. 7A**). Importantly, contrast threshold in CSE mice treated with B4-scFv-fH had significantly improved levels of contrast sensitivity threshold when compared to those treated with empty capsules (smoke+B4-scFv-fH: 18.0 ±2.26; empty capsules versus B4-scFv-fH: $P<0.0001$; **Fig. 7B**) and more similar to those of age-matched never-smokers.

Loss in contrast sensitivity in SIOP has previously been shown to be associated with specific morphological alterations in BrM, and those changes can be prevented in animals without a

functional complement AP ($fB^{-/-}$ mice) (Woodell et al., 2013). Here, we asked whether thickening of BrM can be prevented by treatment with B4-scFv-fH. Transmission electron micrographs obtained from animals treated with empty capsules, capsules containing B4-scFv-fH cells and age-matched never-smokers were compared (**Fig. 7B**). The extent of thickened BrM increased with smoke exposure. Specifically, the percent thickened BrM (>0.28 □m (Annamalai et al., 2020a)) increased to ~60% in smoke exposed mice treated with empty capsules, compared to ~28% in smoke exposed mice treated with capsules containing B4-scFv-fH cells (**Fig. 7D**) (P<0.005). Age-matched never smoked mice had a small amount of thickened BrM of 23% (empty capsules versus B4-scFv-fH: P <0.005; empty capsules versus never smokers: P <0.005; never smokers versus B4-scFv-fH: P =0.49). Overall, there is a good correlation between contrast sensitivity and % thickened BrM among the three groups (R^2=0.6702). Within this thickened BrM (>0.28 □m), an increase in width and area of deposits in the smoke-exposed mice was identified, that was reduced by B4-scFv-fH (empty capsules versus B4-scFv-fH: P <0.001; empty capsules versus never smokers: P <0.003; never smokers versus B4-scFv-fH: P =0.11).

The presence of B4-scFv-fH, complement activation products and antibody binding in the RPE/choroid fractions was assessed by dot blot and Western blotting. As with CNV animals (above), B4-scFv-fH in the RPE/choroid of injected animals was detected (**Fig. 8C)**. Likewise, western blot analyses demonstrated that B4-scFc-fH injected mice had significantly lower levels of C3□' (P <0.05), C3□'1 (P <0.01) and C3dg/C3d (P <0.05) present in the RPE/choroid fraction (**Fig. 8A**). Finally, since B4-scFv-fH binding to neoepitopes in the RPE/choroid is expected to reduce endogenous antibody binding in addition to preventing complement activation, RPE/choroid fractions were analyzed for the presence of IgG and IgM. Significantly

decreased levels of both IgG and IgM were seen in RPE/choroid fractions after 6 months of smoke exposure with B4-scFc-fH treatment when compared to empty capsules (IgM: $P < 0.05$; IgG: $P < 0.001$; **Fig. 8B**). Finally, to confirm the presence of B4-scFv-fH in the RPE/choroid fractions after 6 months, the tissue samples that were probed for the complement activation products and IgG/IgM binding were investigated for the His-tag in the B4-scFv-fH protein using Dot blot analysis (**Fig. 8C**).

DISCUSSION

It has been shown that complement activation is involved in the pathogenesis of human AMD (Anderson et al., 2010; Despriet et al., 2006) as well as in the animal models of wet (Rohrer et al., 2011) and dry AMD (Woodell et al., 2013) examined here. Binding sites for a natural antibody against malondialdehyde (MDA) exist in human eyes with AMD (Weismann et al., 2011), and a natural IgM antibody against the same neoepitope can activate complement on RPE cells (Joseph et al., 2013) and also augment CNV in rag1$^{-/-}$ mice (Joseph et al., 2013). Here, we tested whether a novel IgM mAb that recognizes an annexin IV neoepitope expressed after intestinal, cardiac and cerebral ischemia-reperfusion (Atkinson et al., 2015; Kulik et al., 2009)(Elvington et al., 2012) has a pathogenic role in AMD models, and whether this antibody can be used as a vehicle to deliver a complement inhibitor to damaged ocular tissues. The main results of the current study are: (1) Oxidative stress due to oxidant or smoke exposure generates the annexin IV neoepitope recognized by B4 mAb on ARPE-19 cells; (2) Self-reactive antibodies present in normal serum recognize the B4 annexin IV surface epitope and triggers complement activation; (3) B4 mAb recognizes neoepitopes in CNV lesions, and when injected into antibody-deficient, *rag1*$^{-/-}$ mice increases CNV development; (4) A B4-scFv-fH fusion

protein was generated and confirmed to inhibit complement activation on stressed ARPE-19 cells; (5) Encapsulated ARPE-19 cells stably expressing B4-scFv-fH can be used to provide targeted complement inhibition locally or globally, without inducing an immune response against the drug; (6) B4-scFv-fH produced in the vitreous by the ARPE-19 cells reduces CNV lesion size and reduces CNV-induced increase in complement activation; and (7) B4-scFv-fH produced systemically by ARPE-19 cells reduces SIOP and reduces smoke-induced increase in ocular IgG and IgM binding and complement activation. In summary, these results provide further proof that natural antibodies play an important role in ocular sterile inflammatory conditions such as CNV and SIOP, and further that these antibodies can be used to target a complement inhibitor to sites of inflammation as a means of reducing local complement activation in the eye. From a translational perspective, it is also important to note that an epitope recognized by B4 mAb has been shown to be presented in an injury specific manner in human brain and liver tissue after ischemia and reperfusion (Marshall et al., 2018), but B4 mAb binding has not yet been explored in human donor eyes. And finally, we have shown viability of cell encapsulation method in the SIOP model, a model in which ocular pathology is AP activity-dependent (Woodell et al., 2016). For the inhibitor to gain access to the RPE, Bruch's membrane and choroid in the SIOP model, in which the blood-retina barrier is presumed to be relatively intact, the capsules were delivered subcutaneously, as we have shown previously that inhibitor generated in the vitreous does not reach those structures in intact eyes (Annamalai et al., 2018). Please note that the pros and cons on the use of the ECT technique using alignate capsules were discussed previously (Annamalai et al., 2018), and we only emphasize here again that for use in humans, non-degradable implants like those used by Neurotech, would be used for both intravitreal and extraocular delivery (Tao et al., 2002).

Autoantibodies in disease models

There is evidence that neoepitopes such as malondialdehyde (Weismann et al., 2011) are generated in AMD, that peptides from many different proteins can be found in drusen, (Crabb et al., 2002) and that nAb profiles might correlate with AMD (Morohoshi et al., 2012). While it is unclear how nAbs may contribute to disease, we have generated sufficient data to suggest that binding of nAbs to DMAPs in ocular tissues triggers complement activation, leading to pathology. Here, as well as in previous publications, we have shown that stress can lead to the presentation of neoepitopes on cell surfaces of cells involved in pathology. Specifically, previously we have shown that PC/MDA (recognized by C2 mAb; (Joseph et al., 2013)) is presented on RPE cells stressed with either H_2O_2 or smoke exposure, or in CNV lesions and here we showed the same for annexin IV (B4 mAb). Using a combination of depletion and reconstitution strategies in vitro, we previously demonstrated that the complement activation pathway involved in TER reduction in RPE cells is dependent on ficolin and/or MBL triggering of the LP via antibody-binding to the cell surface (Joseph et al., 2013). In that study we showed that Ig-depleted serum was not sufficient to activate the complement cascade, but reconstitution of the media with IgM-C2 (Joseph et al., 2013) was able to do so. Similarly, we showed previously that Ig-deficient *rag1*$^{-/-}$ mice could be reconstituted with IgM-C2 (Joseph et al., 2013) to increase CNV lesions, whereas a control IgM mAb was ineffective. While in *rag1*$^{-/-}$ mice, this augmentation in CNV lesion size has not been proven to be complement dependent, in C57BL/6J mice, we have shown that mechanism to involve the classical and or lectin pathway for initiation (Rohrer et al., 2011) and the alternative pathway for amplification (Rohrer et al., 2009). Here, we repeated these experiments with IgM B4 and documented the same results in cells and mice.

Thus, we have uncovered a similar mechanism in human RPE cells as well as mouse RPE/choroid whereby which the binding of autoantibodies to DAMPs generated by oxidative stress initiates complement- and VEGF-dependent damage. IgM B4 binding to DAMPs on RPE cells exposed to smoke extracts suggests that a similar mechanism might be involved in smoke-induced ocular pathology (SIOP) induced by long-term second hand smoke exposure. Indeed, in this model, we find dependence of pathology on the alternative pathway (Woodell et al., 2013), C3d-deposition (Woodell et al., 2013), as well as IgM and IgG (IgG1, IgG2a/b and IgG3) binding in RPE, Bruch's membrane and choroid (Annamalai et al., 2020a). While both IgM and IgG can activate the lectin and classical pathway of complement (Muller-Eberhard, 1988), leading to complement dependent cytotoxicity, the different mouse IgG isotypes differ in their capacity to do so (Michaelsen et al., 2004). Likewise, IgGs can interact with Fc□ receptors, triggering antibody-dependent cell-mediated cytotoxicity (ADCC), and again, IgG antibody subtypes differ (Ding et al., 2008). Hence, additional experiments using FcγRIII$^{-/-}$ mice together with the use of complement inhibitors might be able to further distinguish between these two pathways of antibody-dependent cell damage.

Autoantibodies as targeting moieties

We have shown previously that we can target the C3d neoepitopes present in CNV lesions (Rohrer et al., 2009) as well as injured tissue in the SIOP model (Woodell et al., 2016), both therapeutically in form of the fusion protein CR2-fH (Alawieh et al., 2015; Rohrer et al., 2009; Woodell et al., 2016) and for imaging purposes using an antibody against C3d (Thurman et al., 2013). We have now extended this concept targeting a stress-related DAMP, and designed a single-chain variable fragment (scFv) antibody based on IgM B4 fused to the inhibitory domain

of factor H (fH). Proof of concept for this strategy was provided by us previously, using the scFv antibody based on IgM B4 fused to a pan-complement inhibitor (Crry). B4-scFv-Crry was found to significantly reduce neuroinflammation after stroke in mice (Alawieh et al., 2018). Here, B4-scFv-fH was first tested for its ability to bind to stressed RPE cells and to inhibit complement. B4-scFv-fH, which is His tagged, was shown to bind to epitopes generated by H_2O_2 or smoke exposure by anti-His immunohistochemistry (**Fig. 1, bottom row**) on RPE monolayers. Purified B4-scFv-fH protein was shown to reduce complement activation triggered in stressed RPE cell monolayers exposed to H_2O_2 and 10% complement-sufficient normal human serum (**Fig. 2B**), and ARPE-19 cells stably transfected with the B4-scFv-fH construct secrete sufficient amounts of the inhibitor towards the apical side within 48 hours (only time point tested) to protect naïve ARPE-19 cells against complement activation in the same assay.

These ARPE-19 cells stably transfected with the B4-scFv-fH construct were used for therapeutic purposes in two animal models, the short-term angiogenic model of choroidal neovascularization (wet AMD) and the long-term oxidative stress model of smoke-induced ocular pathology. The cell encapsulation technology, together with its pros and cons was discussed by us in a previous publication (Annamalai et al., 2018). In short, we confirmed cell survival in the capsules, long-term secretion of protein, and lack of antibody generation against the active compound, and identified an efficacious number of capsules per eye (Annamalai et al., 2018). Important also for our results here, is that the therapeutic dose of CR2-fH blunted the injury-induced complement activation, but did not reduce complement below baseline or homeostatic levels. Homeostatic levels will allow for both aspects of complement, normal homeostatic functions as well as low level surveillance of the immune system (Ricklin et al., 2010).

ECT-mediated delivery of B4-scFv-fH either intraocularly or systemically resulted in B4-scFv-fH binding to RPE/choroid as show by dot blot analysis. Lower levels of B4-scFv-fH were recovered from equal protein of the retina when compared to the RPE/choroid fraction, presumably since the neoepitopes are generated in the latter tissues (Joseph et al., 2013; Woodell et al., 2013). ECT-mediated delivery of B4-scFv-fH reduced CNV lesion sizes and reduced thickening of BrM and the width and size of the deposits, a surrogate of pathology seen in human (BrM thickening, drusen formation). Likewise, a functional readout, contrast sensitivity was improved. These structural and functional improvements were accompanied by a reduction in IgM, IgG and C3 breakdown products in the RPE/choroid fraction of eyes with CNV or SIOP. A head-to-head comparison between the different targeting moieties (CR2 or B4-scFv) has not yet been performed, and is beyond the scope of this study. However, different outcomes might be anticipated. First, CR2 targets all sites with C3 deposition, including those that might be important for repair as opsonization of tissue is required for removal by macrophages. In contrast, neoepitopes are not known to contribute to repair processes. Second, the CR2 binding site (opsonins) are generated at more distal point in the complement-mediated inflammatory pathway, whereas those for B4-scFv are generated at more proximal point. Third, as complement inhibition is reducing the presence of opsonins, CR2-fH efficacy might be self-limiting, while B4-scFv binds until epitopes until the stressor is eliminated. Fourth, we have shown in mouse that the circulatory half-life of B4-scFv-Crry when compared to CR2-Crry is considerably shorter, which reduces potential systemic effects. Important within the context of systemic safety, DAMP targeting may be less immunosuppressive since not all sites of C3 deposition will be targeted with complement inhibition, exemplified by the observation that B4-scFv-Crry did

not affect host immune resistance to infection in a model of polymicrobial sepsis (Atkinson et al., 2015). Fifth, B4-scFv, unlike CR2 may also increase the fusion protein's therapeutic potential by competing with pathogenic IgM binding to the neoepitopes, which in turn will reduce activation of the LP and CP, which can reduce inflammation, endothelial activation and cell trafficking (Li et al., 2009). Sixth, DAMP-mediated targeting may be more specific for sites of stress/injury since CR2 has been show to also bind to other ligands including IFN□ □(Delcayre et al., 1991), CD23 (Aubry et al., 1992), DNA containing complexes (Holers and Kulik, 2007), Epstein-Barr virus (Lowell et al., 1989), as well as sites of spontaneous complement activation such the extracellular matrix of the choroid (Mullins et al., 2014). Seventh, both functional arms of this kind of construct can be modified in terms of target specificity (Husain and Ellerman, 2018) as well as the complement pathway/product inhibited, making this approach more versatile. And finally, antibody-based therapeutics exhibit intrinsic low toxicity as they are naturally occurring (Fischer and Leger, 2007), although this will have to be confirmed for the

We note that there are limitations to this study. While we have shown that IgM-B4 can augment CNV in rag1$^{-/-}$ mice, the same needs to be completed for the SIOP model. We have not specifically addressed how complement inhibition reduces angiogenesis and BrM thickness, other than to speculate that the mechanism occurs in an IgG/IgM dependent manner. B4-scFv-fH also reduces anaphylatoxin generation; in the present study, we only measured the levels of C3a, but not C5a anaphylatoxins generated, and did not address their role in contributing to pathogenesis. IgM B4 is the second neoepitope we have examined in the context of the mouse CNV model (IgM C2); it would be of great interest to determine whether C2-scFv-fH would

provide better protection than B4-scFv-fH, or whether targeting the two neoepitopes should be combined. Nevertheless, we provided evidence that the B4 neoepitope is present on both human and mouse target cells, and that B4-scFv can be used effectively to deliver the AP-inhibitor factor H to sites of complement activation in the eye, reducing complement activation, IgG/IgM deposition and resulting pathology long-term.

Acknowledgements

At MUSC, the study was supported by the National Institutes of Health (NIH) (R01EY019320, R01EY024581) (BR), the Department of Veterans Affairs (IK6BX004858, RX000444 and BX003050) (BR), (IK6BX005235, RX001141 and BX004256) (ST), and the South Carolina SmartState Endowment (BR). In Utah, the following grants are acknowledged: R01 EY015128 (BWJ, R01 EY028927 to BWJ, P30 EY014800 to Moran Eye Center Core, and Research to Prevent Blindness (New York) Unrestricted Grant to the Department of Ophthalmology & Visual Sciences, University of Utah.

Conflict of interest

BR and ST are inventors on patents that describe the B4-fH technology. The remaining authors declare that they have no conflict of interest.

Figure Legends

Figure 1. B4 neoepitopes (modified annexin IV) are present on oxidatively stressed, but not healthy, ARPE-19 cells. Top row. Immunofluorescence staining of ARPE cells using the B4 IgM antibody in the presence and absence of H_2O_2 or 10% smoke extract. Specific staining was revealed in oxidatively stressed cells when compared to control (healthy) cells. Incubation without primary antibody was performed as a negative control. **Bottom row.** The B4-scFv-fH (B4-fH) similarly recognized epitopes present on stressed ARPE cells.

Figure 2. Complement activation on stressed cells requires natural antibodies. (**A**) TER measurements were performed using 10% complement sufficient serum (complete) as well as 10% serum from which all antibodies were depleted (Ig-depleted [Igd] normal human serum [NHS]). TER is reduced in by complement activation (elicited by complete NHS in the presence of oxidative stress [0.5 mM H_2O_2]) as shown previously (Thurman et al., 2009). Reduction in TER is obliterated in Ig-depleted serum (Joseph et al., 2013). Reconstitution with the IgM natural antibody B4, activated the complement cascade in this assay, whereas the control IgM antibody was ineffective. (**B**) Media from ARPE-19 monolayers stably transfected with B4-scFv-fH plasmid or control cells was collected after a 48 hour secretion period. B4-scFv-fH protein containing media or control media was transferred to new monolayers prior to complement activation by 5% complete NHS and 0.5 mM H_2O_2. The amount of B4-scFv-fH protein secreted

was sufficient to protect against complement activation when compared to control. Data (mean ±SEM) representing wells from 3 independent experiments are shown.

Figure 3. B4 neoepitopes are generated in CNV lesions and IgM-B4 mAb augments lesion size when administered to rag1$^{-/-}$ mice. (A) Immunofluorescence staining of CNV lesions using IgM B4 mAb and control mAb. **(B)** Antibody-deficient *rag1*$^{-/-}$ mice were reconstituted with three injections of IgM B4 or control IgM during the course of CNV development. IgM B4 injections resulted in a significant increase in lesion size when compared to the control antibody. Lesion sizes (volume) were assessed using isolectin-B4 staining in RPE/choroid flatmounts. Data (mean ± SEM) representing spots from 6 animals per group are shown.

Figure 4. Encapsulated cell technology to deliver B4-scFv-fH. (**A**) ARPE-19 cells stably expressing B4-scFv-fH were encapsulated in alginate as published (Annamalai et al., 2018). **Top row**. Supernatant from encapsulated cells was collected and a dilution series probed for the presence of B4-scFv-fH using an antibody against the His tag. **Bottom row**. Stably transfected ARPE-19 cells secrete B4-scFv-fH towards both the apical and basal side when grown as monolayers on transwell plates (supernatants from 3 different cultures). (**B**) Long-term systemic B4-scFv-fH expression does not result in systemic response. Seven month following deposition on capsules containing ARPE-19 cells stably expressing B4-scFv-fH, or empty capsules, sera was collected. Three concentrations of cell supernatants from (A) (20, 25 and 30 □L) were probed with a His-tag specific antibody to identify the molecular weight of B4-scFv-fH (72-75 kDa) protein in control lanes (panel 1). Two concentrations of supernatant (20 and 30 mL) were

probed with sera from mice injected with either B4-scFv-fH (panels 2 and 3) or empty capsules (panels 4 and 5) as a source of primary antibody and with either IgG or IgM as a secondary antibody.

Figure 5. Effects of intravitreal delivery of B4-scFv-fH on CNV development. ARPE-19 cells stably expressing B4-scFv-fH were encapsulated in alginate and delivered intravitreally as published (Annamalai et al., 2018). (**A**) B4-scFv-fH capsule treatment resulted in a significant decrease in lesion size when compared to treatment with empty capsules. (**B**) Lesion sizes (diameter) assessed using OCT images, demonstrating efficacy of B4-scFv-fH at reducing lesion size. Data are expressed as mean ± SEM (n = 12).

Figure 6. Effects of intravitreal delivery of B4-scFv-fH on complement activation, IgM/IgG deposition. (**A**) Dot blots of RPE/choroid and retina samples from B4-scFv-fH treated and empty capsule treated mice 6 days after CNV induction. Two independent samples per condition were probed for the presence of B4-scFv-fH using anti-His-tag antibody, confirming expression of B4-scFv-fH from the ARPE-19 cells in the vitreous and retention of the inhibitor in RPE/choroid. (**B, B'**) Western blot and band density analysis of complement activation. Equal amounts of RPE/choroid extracts (15 □g/lane) were loaded per lane, probed for the C3d domain present in the C3□ chain and its breakdown products (Thurman et al., 2013), and band intensities quantified. Arbitrary values were established based on normalization with □-actin. All breakdown products of C3□, identified according to MW (C3□', C3□'1 and C3dg/C3d), were significantly reduced in B4-scFv-fH treated animals compared to empty capsule treated animals.

(**C**) C3a, as assessed by ELISA revealed a significant increase in C3a after CNV induction in the empty capsule-treated mice, which was normalized to baseline levels in the B4-scFv-fH treated group. (**D, D'**) Western blot and band density analysis of antibody deposition. IgG and IgM levels were elevated by CNV and reduced in B4-scFv-fH treated mice. Data are expressed as mean ± SEM (n = 5 independent samples per condition for protein analysis, and 3 independent samples are shown per condition in Western blots).

Figure 7. Effects of systemic delivery of B4-scFv-fH on visual function and Bruch's membrane thickness in the SIOP model. (**A**) Contrast sensitivity was measured by measuring the contrast threshold at a fixed spatial frequency (0.131 cyc/deg) and speed (12 deg/sec). We previously determined that this spatial frequency falls within the range of maximal contrast sensitivity for 9-month-old WT mice (data not shown). Smoke exposed mice showed a significant reduction in contrast sensitivity compared to controls exposed to room air, which was prevented in mice treated with B4-scFv-fH. (**B**) Transmission electron micrographs of the RPE obtained from C57BL/6J mice exposed to 6 months of smoke in the absence (empty) and presence of B4-scFv-fH (B4-scFv-fH). The RPE/BrM/CC in animals exposed to smoke exhibit pathological changes, including a thickening of BrM, which becomes disorganized, and loses its pentalaminar structure at its ticker points. (**C**) BrM thickness was examined and the percent BrM along a given RPE cell that is damaged (exceed the normal thickness [<0.28 □m] (Annamalai et al., 2020a) of BrM in age-matched room air exposed mice (Annamalai et al., 2020a)) is established. (**D**) In addition, width of BrM deposits (see arrowhead in C) and their area was determined. For all three features, a smoke exposure and treatment effect is demonstrated. Data are expressed as mean ± SEM (n = 4-5 eyes per condition).

Figure 8. Effects of systemic delivery of B4-scFv-fH on complement activation, IgM/IgG deposition and B4-scFv-fH binding in RPE/choroid of the SIOP model. (**A, A'**) Western blot and corresponding band density analysis of complement activation. Equal amounts of RPE/choroid extracts (15 □g/lane) were loaded per lane, probed for the C3d domain, and band intensities quantified. Arbitrary values were established based on normalization with □-actin. All breakdown products of C3□, identified according to MW (C3□', C3□'1 and C3dg/C3d), were significantly reduced in B4-scFv-fH treated animals compared to empty capsule treated animals. (**B, B'**) Western blot and band density analysis of antibody deposition. IgG and IgM levels were elevated in smoke exposed mice and reduced in B4-scFv-fH treated smoke exposed mice. (**C**) Dot blots of RPE/choroid and retina samples from B4-scFv-fH treated and empty capsule treated mice. Samples were probed for the presence of B4-scFv-fH using anti-His-tag antibody, confirming expression of B4-scFv-fH. Data are expressed as mean ± SEM (n = 4-5 independent samples per condition for protein analysis, and 3 independent samples are shown per consition in Western blots).

REFERENCES

Ablonczy, Z., Crosson, C.E., 2007. VEGF modulation of retinal pigment epithelium resistance. Exp Eye Res 85, 762-771.
Alawieh, A., Elvington, A., Zhu, H., Yu, J., Kindy, M.S., Atkinson, C., Tomlinson, S., 2015. Modulation of post-stroke degenerative and regenerative processes and subacute protection by site-targeted inhibition of the alternative pathway of complement. J Neuroinflammation 12, 247.
Alawieh, A., Langley, E.F., Tomlinson, S., 2018. Targeted complement inhibition salvages stressed neurons and inhibits neuroinflammation after stroke in mice. Sci Transl Med 10.
Anderson, D.H., Radeke, M.J., Gallo, N.B., Chapin, E.A., Johnson, P.T., Curletti, C.R., Hancox, L.S., Hu, J., Ebright, J.N., Malek, G., Hauser, M.A., Rickman, C.B., Bok, D., Hageman, G.S.,

Johnson, L.V., 2010. The pivotal role of the complement system in aging and age-related macular degeneration: hypothesis re-visited. Prog Retin Eye Res 29, 95-112.
Anderson, J.R., Jones, B.W., Yang, J.H., Shaw, M.V., Watt, C.B., Koshevoy, P., Spaltenstein, J., Jurrus, E., U, V.K., Whitaker, R.T., Mastronarde, D., Tasdizen, T., Marc, R.E., 2009. A computational framework for ultrastructural mapping of neural circuitry. PLoS Biol 7, e1000074.
Annamalai, B., Nicholson, C., Parsons, N., Stephenson, S., Atkinson, C., Jones, B., Rohrer, B., 2020a. Immunization Against Oxidized Elastin Exacerbates Structural and Functional Damage in Mouse Model of Smoke-Induced Ocular Injury. Invest Ophthalmol Vis Sci 61, 45.
Annamalai, B., Parsons, N., Belhaj, M., Brandon, C., Potts, J., Rohrer, B., 2018. Encapsulated Cell Technology-Based Delivery of a Complement Inhibitor Reduces Choroidal Neovascularization in a Mouse Model. Transl Vis Sci Technol 7, 3.
Annamalai, B., Parsons, N., Brandon, C., Rohrer, B., 2020b. The use of matrigel combined with encapsulated cell technology to deliver a complement inhibitor in a mouse model of choroidal neovascularization. . Mol Vision in press.
Atkinson, C., Qiao, F., Yang, X., Zhu, P., Reaves, N., Kulik, L., Goddard, M., Holers, V.M., Tomlinson, S., 2015. Targeting pathogenic postischemic self-recognition by natural IgM to protect against posttransplantation cardiac reperfusion injury. Circulation 131, 1171-1180.
Atkinson, C., Song, H., Lu, B., Qiao, F., Burns, T.A., Holers, V.M., Tsokos, G.C., Tomlinson, S., 2005. Targeted complement inhibition by C3d recognition ameliorates tissue injury without apparent increase in susceptibility to infection. J Clin Invest 115, 2444-2453.
Aubry, J.P., Pochon, S., Graber, P., Jansen, K.U., Bonnefoy, J.Y., 1992. CD21 is a ligand for CD23 and regulates IgE production. Nature 358, 505-507.
Bandyopadhyay, M., Rohrer, B., 2012. Matrix metalloproteinase activity creates pro-angiogenic environment in primary human retinal pigment epithelial cells exposed to complement. Invest Ophthalmol Vis Sci 53, 1953-1961.
Baumgarth, N., Tung, J.W., Herzenberg, L.A., 2005. Inherent specificities in natural antibodies: a key to immune defense against pathogen invasion. Springer Semin Immunopathol 26, 347-362.
Belhaj, M., Annamalai, B., Parsons, N., Shuler, A., Potts, J., Rohrer, B., 2020. Encapsulated Cell Technology for the Delivery of Biologics to the Mouse Eye. J Vis Exp.
Brown, M.M., Brown, G.C., Stein, J.D., Roth, Z., Campanella, J., Beauchamp, G.R., 2005. Age-related macular degeneration: economic burden and value-based medicine analysis. Can J Ophthalmol 40, 277-287.
Campa, C., Kasman, I., Ye, W., Lee, W.P., Fuh, G., Ferrara, N., 2008. Effects of an anti-VEGF-A monoclonal antibody on laser-induced choroidal neovascularization in mice: optimizing methods to quantify vascular changes. Invest Ophthalmol Vis Sci 49, 1178-1183.
Chen, Y., Park, Y.B., Patel, E., Silverman, G.J., 2009. IgM antibodies to apoptosis-associated determinants recruit C1q and enhance dendritic cell phagocytosis of apoptotic cells. J Immunol 182, 6031-6043.
Clark, S.J., Bishop, P.N., 2018. The eye as a complement dysregulation hotspot. Semin Immunopathol 40, 65-74.
Coughlin, B., Schnabolk, G., Joseph, K., Raikwar, H., Kunchithapautham, K., Johnson, K., Moore, K., Wang, Y., Rohrer, B., 2016. Connecting the innate and adaptive immune responses in mouse choroidal neovascularization via the anaphylatoxin C5a and gammadeltaT-cells. Sci Rep 6, 23794.
Crabb, J.W., Miyagi, M., Gu, X., Shadrach, K., West, K.A., Sakaguchi, H., Kamei, M., Hasan, A., Yan, L., Rayborn, M.E., Salomon, R.G., Hollyfield, J.G., 2002. Drusen proteome analysis: an

approach to the etiology of age-related macular degeneration. Proc Natl Acad Sci USA 99, 14682-14687.
Delcayre, A.X., Salas, F., Mathur, S., Kovats, K., Lotz, M., Lernhardt, W., 1991. Epstein Barr virus/complement C3d receptor is an interferon alpha receptor. Embo J 10, 919-926.
Despriet, D.D., Klaver, C.C., Witteman, J.C., Bergen, A.A., Kardys, I., de Maat, M.P., Boekhoorn, S.S., Vingerling, J.R., Hofman, A., Oostra, B.A., Uitterlinden, A.G., Stijnen, T., van Duijn, C.M., de Jong, P.T., 2006. Complement factor H polymorphism, complement activators, and risk of age-related macular degeneration. JAMA 296, 301-309.
Ding, J.W., Zhou, T., Zeng, H., Ma, L., Verbeek, J.S., Yin, D., Shen, J., Chong, A.S., 2008. Hyperacute rejection by anti-Gal IgG1, IgG2a, and IgG2b is dependent on complement and Fc-gamma receptors. J Immunol 180, 261-268.
Elkon, K., Casali, P., 2008. Nature and functions of autoantibodies. Nat Clin Pract Rheumatol 4, 491-498.
Elvington, A., Atkinson, C., Kulik, L., Zhu, H., Yu, J., Kindy, M.S., Holers, V.M., Tomlinson, S., 2012. Pathogenic natural antibodies propagate cerebral injury following ischemic stroke in mice. J Immunol 188, 1460-1468.
Fearon, D.T., 1998. The complement system and adaptive immunity. Semin Immunol 10, 355-361.
Fischer, N., Leger, O., 2007. Bispecific antibodies: molecules that enable novel therapeutic strategies. Pathobiology 74, 3-14.
Giani, A., Thanos, A., Roh, M.I., Connolly, E., Trichonas, G., Kim, I., Gragoudas, E., Vavvas, D., Miller, J.W., 2011. In vivo evaluation of laser-induced choroidal neovascularization using spectral-domain optical coherence tomography. Invest Ophthalmol Vis Sci 52, 3880-3887.
Gu, X., Meer, S.G., Miyagi, M., Rayborn, M.E., Hollyfield, J.G., Crabb, J.W., Salomon, R.G., 2003. Carboxyethylpyrrole protein adducts and autoantibodies, biomarkers for age-related macular degeneration. J Biol Chem 278, 42027-42035.
Holers, V.M., 2000. Phenotypes of complement knockouts. Immunopharmacology 49, 125-131.
Holers, V.M., 2003. The complement system as a therapeutic target in autoimmunity. Clin Immunol 107, 140-151.
Holers, V.M., Kulik, L., 2007. Complement receptor 2, natural antibodies and innate immunity: Inter-relationships in B cell selection and activation. Molecular immunology 44, 64-72.
Holers, V.M., Rohrer, B., Tomlinson, S., 2013. CR2-mediated targeting of complement inhibitors: bench-to-bedside using a novel strategy for site-specific complement modulation. Adv Exp Med Biol 735, 137-154.
Hollyfield, J.G., Perez, V.L., Salomon, R.G., 2010. A hapten generated from an oxidation fragment of docosahexaenoic acid is sufficient to initiate age-related macular degeneration. Mol Neurobiol 41, 290-298.
Husain, B., Ellerman, D., 2018. Expanding the Boundaries of Biotherapeutics with Bispecific Antibodies. BioDrugs 32, 441-464.
Joachim, S.C., Bruns, K., Lackner, K.J., Pfeiffer, N., Grus, F.H., 2007. Analysis of IgG antibody patterns against retinal antigens and antibodies to alpha-crystallin, GFAP, and alpha-enolase in sera of patients with "wet" age-related macular degeneration. Graefes Arch Clin Exp Ophthalmol 245, 619-626.
Joseph, K., Kulik, L., Coughlin, B., Kunchithapautham, K., Bandyopadhyay, M., Thiel, S., Thielens, N.M., Holers, V.M., Rohrer, B., 2013. Oxidative Stress Sensitizes RPE Cells to

Complement-Mediated Injury in a Natural Antibody-, Lectin Pathway- and Phospholipid Epitope-Dependent Manner. J Biol Chem.
Kulik, L., Fleming, S.D., Moratz, C., Reuter, J.W., Novikov, A., Chen, K., Andrews, K.A., Markaryan, A., Quigg, R.J., Silverman, G.J., Tsokos, G.C., Holers, V.M., 2009. Pathogenic natural antibodies recognizing annexin IV are required to develop intestinal ischemia-reperfusion injury. J Immunol 182, 5363-5373.
Kunchithapautham, K., Atkinson, C., Rohrer, B., 2014. Smoke Exposure Causes Endoplasmic Reticulum Stress and Lipid Accumulation in Retinal Pigment Epithelium through Oxidative Stress and Complement Activation. J Biol Chem 289, 14534-14546.
Li, Y., Wang, H., Peng, J., Gibbs, R.A., Lewis, R.A., Lupski, J.R., Mardon, G., Chen, R., 2009. Mutation survey of known LCA genes and loci in the Saudi Arabian population. Invest Ophthalmol Vis Sci 50, 1336-1343.
Lowell, C.A., Klickstein, L.B., Carter, R.H., Mitchell, J.A., Fearon, D.T., Ahearn, J.M., 1989. Mapping of the Epstein-Barr virus and C3dg binding sites to a common domain on complement receptor type 2. J Exp Med 170, 1931-1946.
Marshall, K., Jin, J., Atkinson, C., Alawieh, A., Qiao, F., Lei, B., Chavin, K.D., He, S., Tomlinson, S., 2018. Natural immunoglobulin M initiates an inflammatory response important for both hepatic ischemia reperfusion injury and regeneration in mice. Hepatology 67, 721-735.
Michaelsen, T.E., Kolberg, J., Aase, A., Herstad, T.K., Hoiby, E.A., 2004. The four mouse IgG isotypes differ extensively in bactericidal and opsonophagocytic activity when reacting with the P1.16 epitope on the outer membrane PorA protein of Neisseria meningitidis. Scand J Immunol 59, 34-39.
Morohoshi, K., Patel, N., Ohbayashi, M., Chong, V., Grossniklaus, H.E., Bird, A.C., Ono, S.J., 2012. Serum autoantibody biomarkers for age-related macular degeneration and possible regulators of neovascularization. Exp Mol Pathol 92, 64-73.
Muller-Eberhard, H.J., 1988. Molecular organization and function of the complement system. Annu Rev Biochem 57, 321-347.
Mullins, R.F., Schoo, D.P., Sohn, E.H., Flamme-Wiese, M.J., Workamelahu, G., Johnston, R.M., Wang, K., Tucker, B.A., Stone, E.M., 2014. The membrane attack complex in aging human choriocapillaris: relationship to macular degeneration and choroidal thinning. Am J Pathol 184, 3142-3153.
Nozaki, M., Raisler, B.J., Sakurai, E., Sarma, J.V., Barnum, S.R., Lambris, J.D., Chen, Y., Zhang, K., Ambati, B.K., Baffi, J.Z., Ambati, J., 2006a. Drusen complement components C3a and C5a promote choroidal neovascularization. Proceedings of the National Academy of Sciences of the United States of America 103, 2328-2333.
Nozaki, M., Raisler, B.J., Sakurai, E., Sarma, J.V., Barnum, S.R., Lambris, J.D., Chen, Y., Zhang, K., Ambati, B.K., Baffi, J.Z., Ambati, J., 2006b. Drusen complement components C3a and C5a promote choroidal neovascularization. Proc Natl Acad Sci USA 103, 2328-2333.
Ozkan, B., Karabas, L.V., Altintas, O., Tamer, G.S., Yuksel, N., Caglar, Y., 2012. Plasma antiphospholipid antibody levels in age-related macular degeneration. Can J Ophthalmol 47, 264-268.
Patel, N., Ohbayashi, M., Nugent, A.K., Ramchand, K., Toda, M., Chau, K.Y., Bunce, C., Webster, A., Bird, A.C., Ono, S.J., Chong, V., 2005. Circulating anti-retinal antibodies as immune markers in age-related macular degeneration. Immunology 115, 422-430.
Rayborn, M.E., Sakaguchi, H., Shadrach, K.G., Crabb, J.W., Hollyfield, J.G., 2006. Annexins in Bruch's membrane and drusen. Adv Exp Med Biol 572, 75-78.

Reuter, J., 2011. Subcutaneous Injection of Tumor Cells. Bio-101, e166.
Ricklin, D., Hajishengallis, G., Yang, K., Lambris, J.D., 2010. Complement: a key system for immune surveillance and homeostasis. Nat Immunol 11, 785-797.
Rohrer, B., Coughlin, B., Bandyopadhyay, M., Holers, V.M., 2012. Systemic Human CR2-Targeted Complement Alternative Pathway Inhibitor Ameliorates Mouse Laser-Induced Choroidal Neovascularization. J Ocul Pharmacol Ther.
Rohrer, B., Coughlin, B., Kunchithapautham, K., Long, Q., Tomlinson, S., Takahashi, K., Holers, V.M., 2011. The alternative pathway is required, but not alone sufficient, for retinal pathology in mouse laser-induced choroidal neovascularization. Mol Immunol 48, e1-8.
Rohrer, B., Long, Q., Coughlin, B., Wilson, R.B., Huang, Y., Qiao, F., Tang, P.H., Kunchithapautham, K., Gilkeson, G.S., Tomlinson, S., 2009. A targeted inhibitor of the alternative complement pathway reduces angiogenesis in a mouse model of age-related macular degeneration. Invest Ophthalmol Vis Sci 50, 3056-3064.
Saeed, A.F., Wang, R., Ling, S., Wang, S., 2017. Antibody Engineering for Pursuing a Healthier Future. Front Microbiol 8, 495.
Schnabolk, G., Coughlin, B., Joseph, K., Kunchithapautham, K., Bandyopadhyay, M., O'Quinn, E., Nowling, T., Rohrer, B., 2015. Local production of the alternative pathway component, Factor B, is sufficient to promote laser-induced choroidal neovascularization. Investigative ophthalmology & visual science.
Schnabolk, G., Stauffer, K., O'Quinn, E., Coughlin, B., Kunchithapautham, K., Rohrer, B., 2014. A comparative analysis of C57BL/6J and 6N substrains; chemokine/cytokine expression and susceptibility to laser-induced choroidal neovascularization. Exp Eye Res 129, 18-23.
Scholl, H.P., Charbel Issa, P., Walier, M., Janzer, S., Pollok-Kopp, B., Borncke, F., Fritsche, L.G., Chong, N.V., Fimmers, R., Wienker, T., Holz, F.G., Weber, B.H., Oppermann, M., 2008. Systemic complement activation in age-related macular degeneration. PLoS ONE 3, e2593.
Sieving, P.A., 2005. NEI Symposium: Age-Related Macular Degeneration (AMD) and Complement Factor H. NIH Videocast June 14.
Silverman, G.J., Gronwall, C., Vas, J., Chen, Y., 2009. Natural autoantibodies to apoptotic cell membranes regulate fundamental innate immune functions and suppress inflammation. Discov Med 8, 151-156.
Stoppelkamp, S., Riedel, G., Platt, B., 2010. Culturing conditions determine neuronal and glial excitability. J Neurosci Methods 194, 132-138.
Tan, P.L., Bowes Rickman, C., Katsanis, N., 2016. AMD and the alternative complement pathway: genetics and functional implications. Hum Genomics 10, 23.
Tao, W., Wen, R., Goddard, M.B., Sherman, S.D., O'Rourke, P.J., Stabila, P.F., Bell, W.J., Dean, B.J., Kauper, K.A., Budz, V.A., Tsiaras, W.G., Acland, G.M., Pearce-Kelling, S., Laties, A.M., Aguirre, G.D., 2002. Encapsulated cell-based delivery of CNTF reduces photoreceptor degeneration in animal models of retinitis pigmentosa. Invest Ophthalmol Vis Sci 43, 3292-3298.
Thurman, J.M., Kulik, L., Orth, H., Wong, M., Renner, B., Sargsyan, S.A., Mitchell, L.M., Hourcade, D.E., Hannan, J.P., Kovacs, J.M., Coughlin, B., Woodell, A.S., Pickering, M.C., Rohrer, B., Holers, V.M., 2013. Detection of complement activation using monoclonal antibodies against C3d. J Clin Invest 123, 2218-2230.
Thurman, J.M., Renner, B., Kunchithapautham, K., Ferreira, V.P., Pangburn, M.K., Ablonczy, Z., Tomlinson, S., Holers, V.M., Rohrer, B., 2009. Oxidative stress renders retinal pigment epithelial cells susceptible to complement-mediated injury. J Biol Chem 284, 16939-16947.

Umeda, S., Suzuki, M.T., Okamoto, H., Ono, F., Mizota, A., Terao, K., Yoshikawa, Y., Tanaka, Y., Iwata, T., 2005. Molecular composition of drusen and possible involvement of anti-retinal autoimmunity in two different forms of macular degeneration in cynomolgus monkey (Macaca fascicularis). Faseb J 19, 1683-1685.
Weismann, D., Hartvigsen, K., Lauer, N., Bennett, K.L., Scholl, H.P., Charbel Issa, P., Cano, M., Brandstatter, H., Tsimikas, S., Skerka, C., Superti-Furga, G., Handa, J.T., Zipfel, P.F., Witztum, J.L., Binder, C.J., 2011. Complement factor H binds malondialdehyde epitopes and protects from oxidative stress. Nature 478, 76-81.
Woodell, A., Coughlin, B., Kunchithapautham, K., Casey, S., Williamson, T., Ferrell, W.D., Atkinson, C., Jones, B.W., Rohrer, B., 2013. Alternative complement pathway deficiency ameliorates chronic smoke-induced functional and morphological ocular injury. PLoS ONE 8, e67894.
Woodell, A., Jones, B.W., Williamson, T., Schnabolk, G., Tomlinson, S., Atkinson, C., Rohrer, B., 2016. A Targeted Inhibitor of the Alternative Complement Pathway Accelerates Recovery From Smoke-Induced Ocular Injury. Invest Ophthalmol Vis Sci 57, 1728-1737.

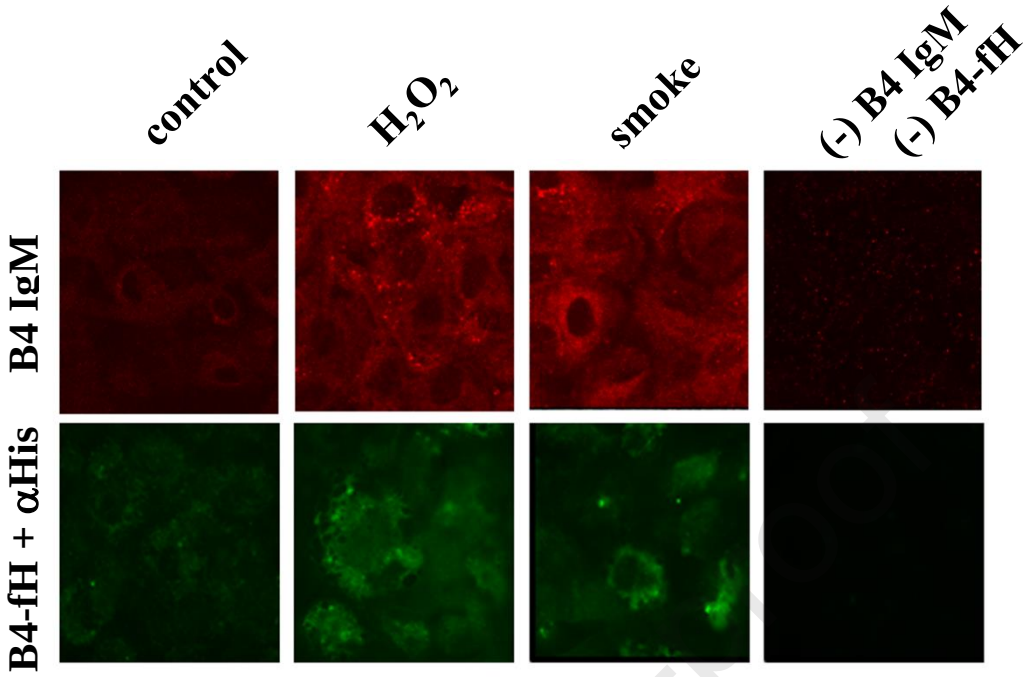

A

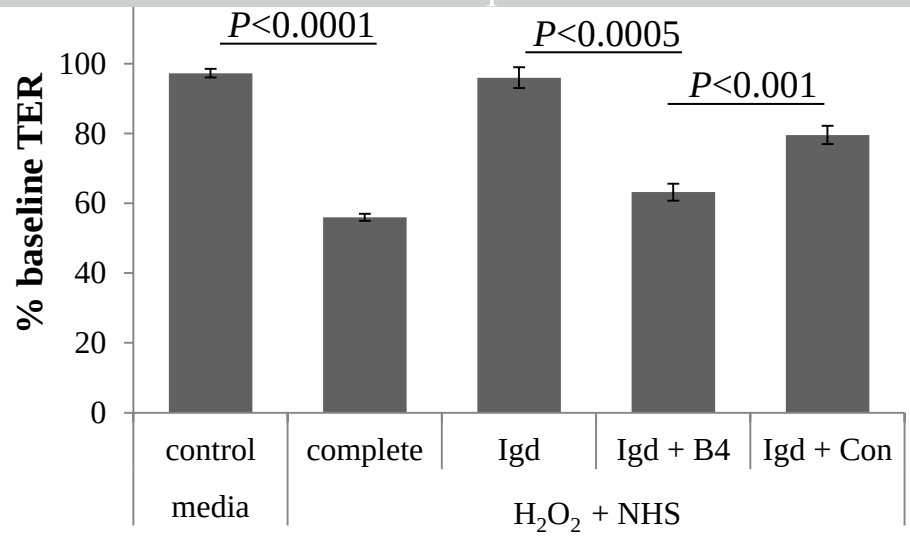

B

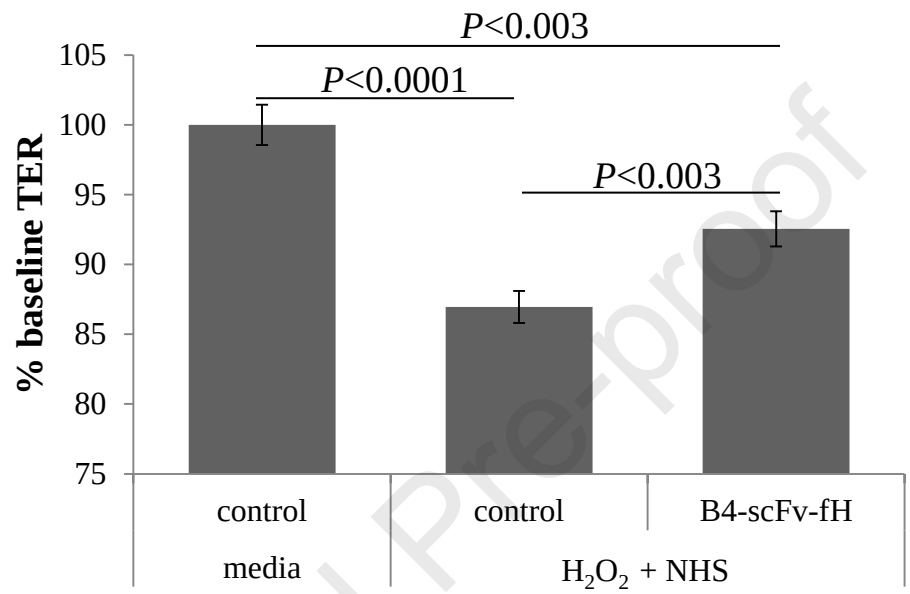

A

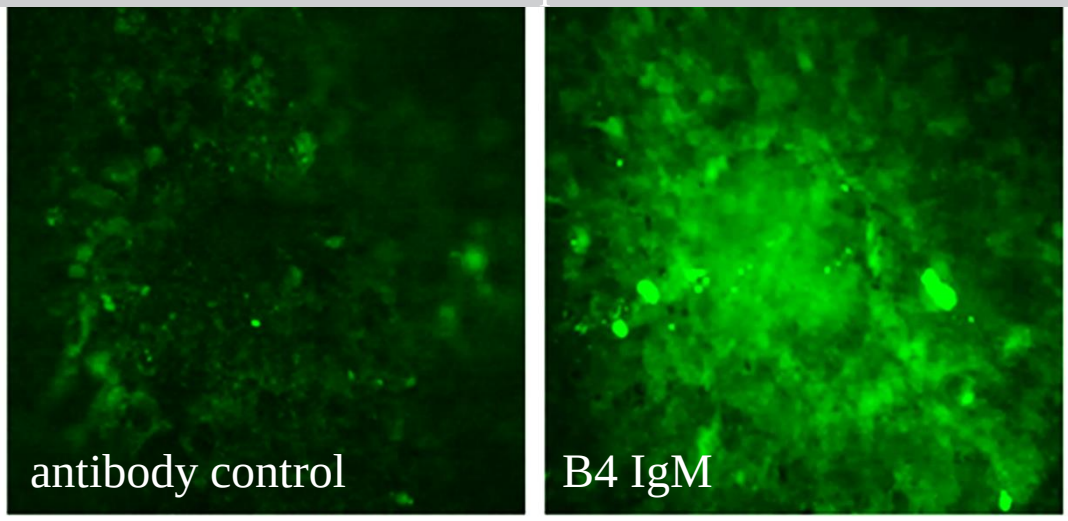

B

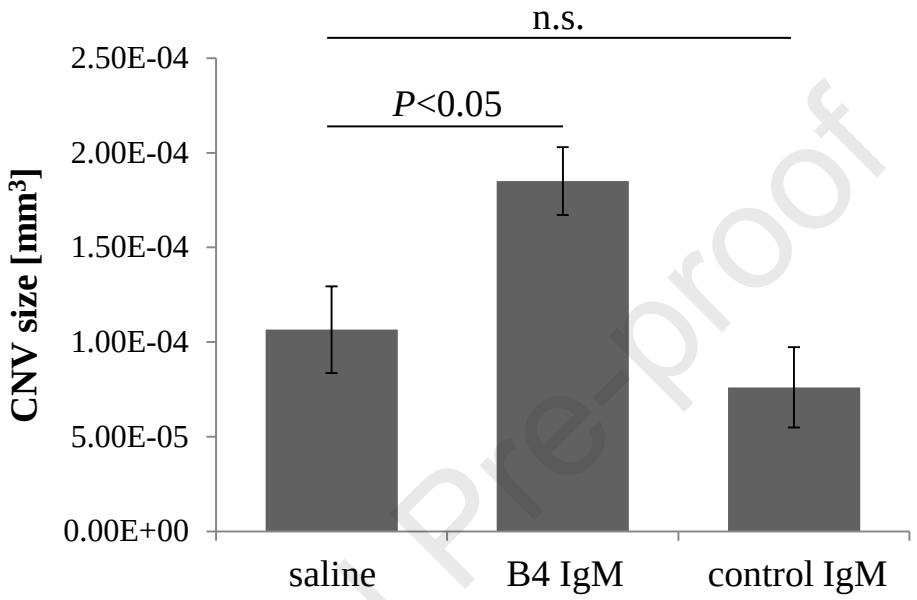

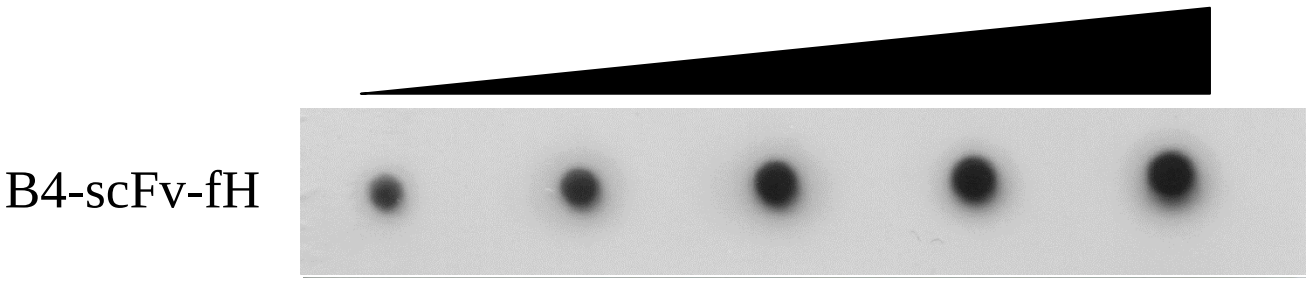

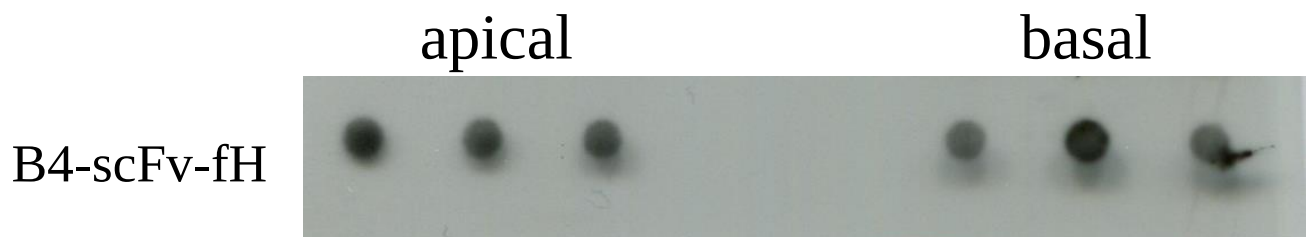

B

primary antibody	His	B4-scFv-fH	B4-scFv-fH	empty	empty
secondary antibody	IgG	IgG	IgM	IgG	IgM

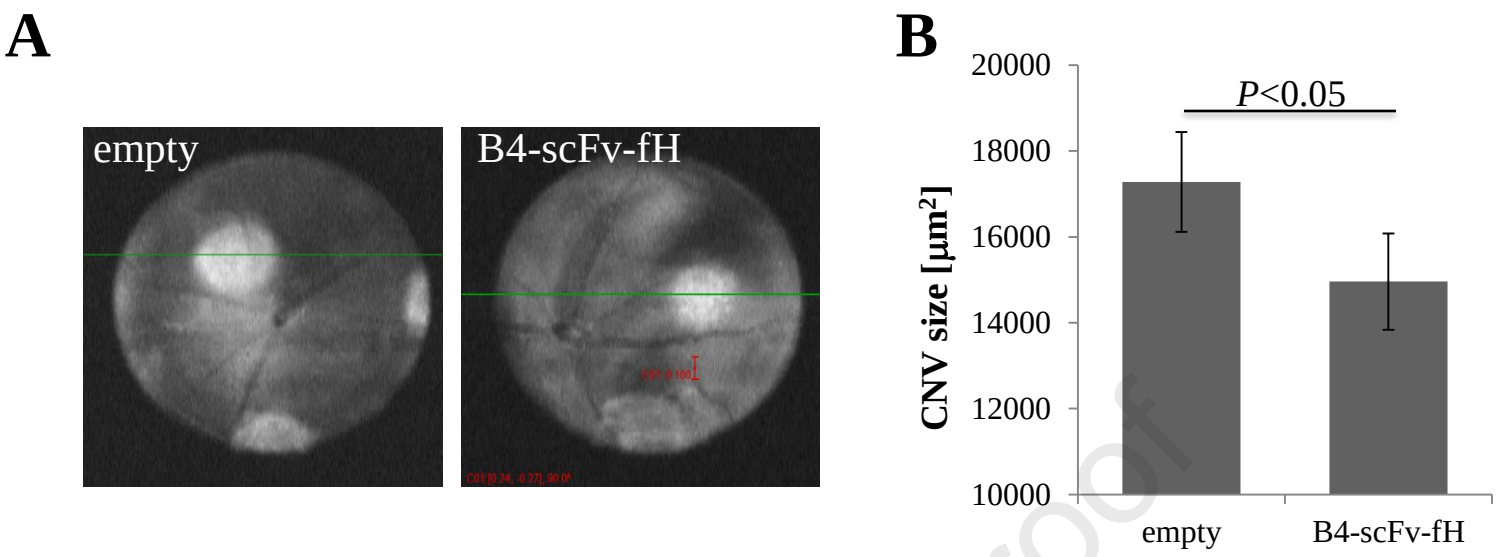

A

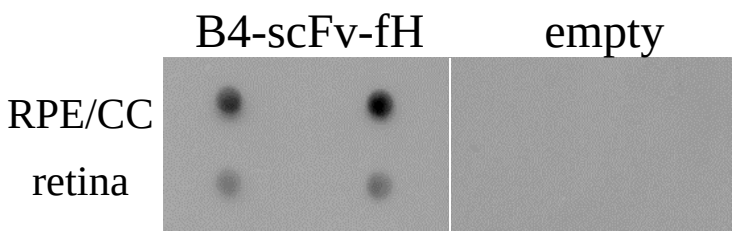

C

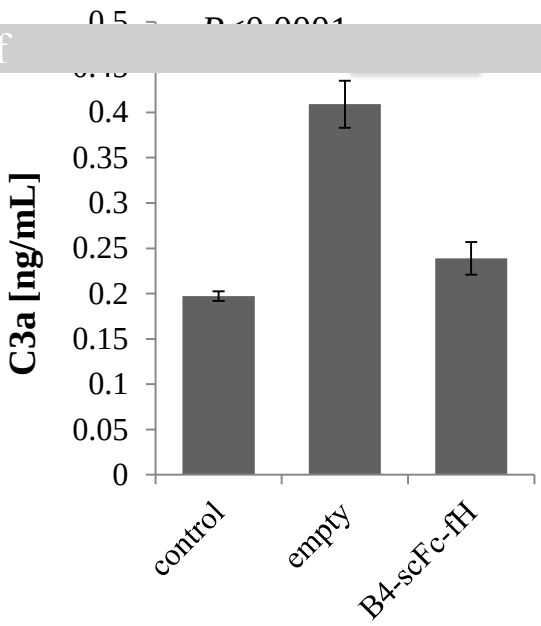

B

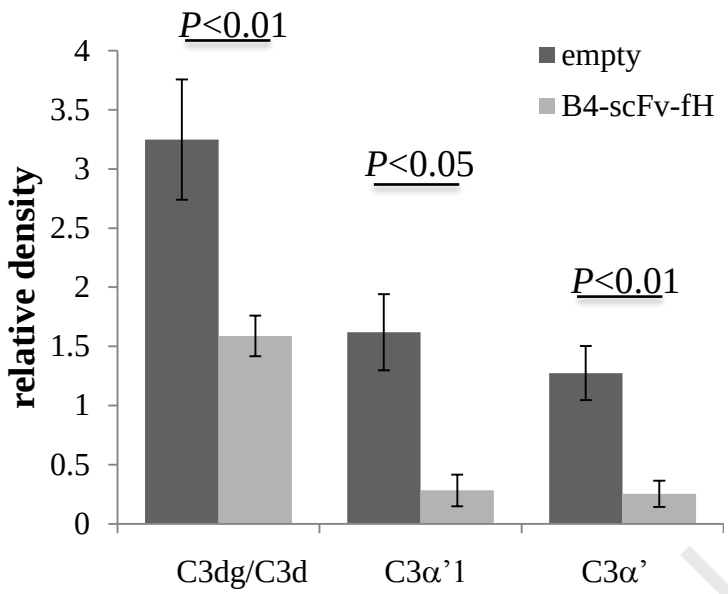

D

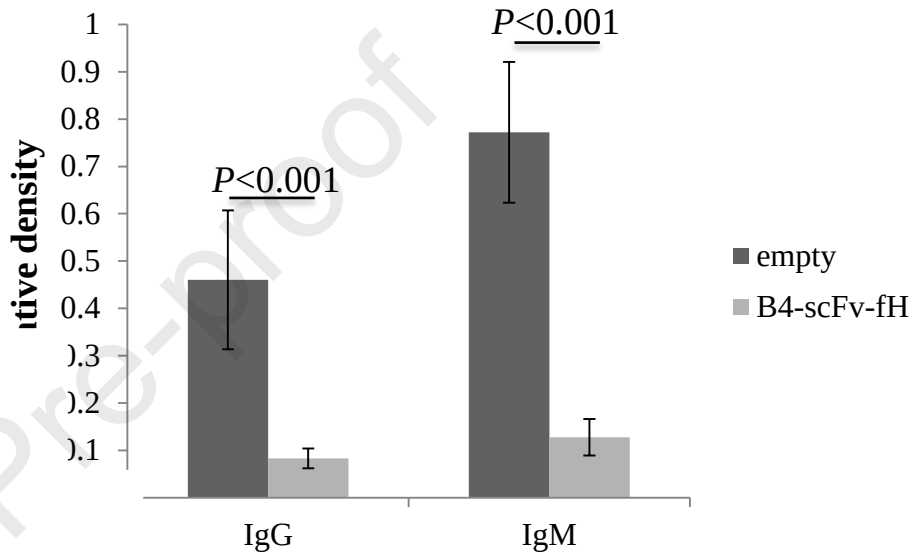

B'

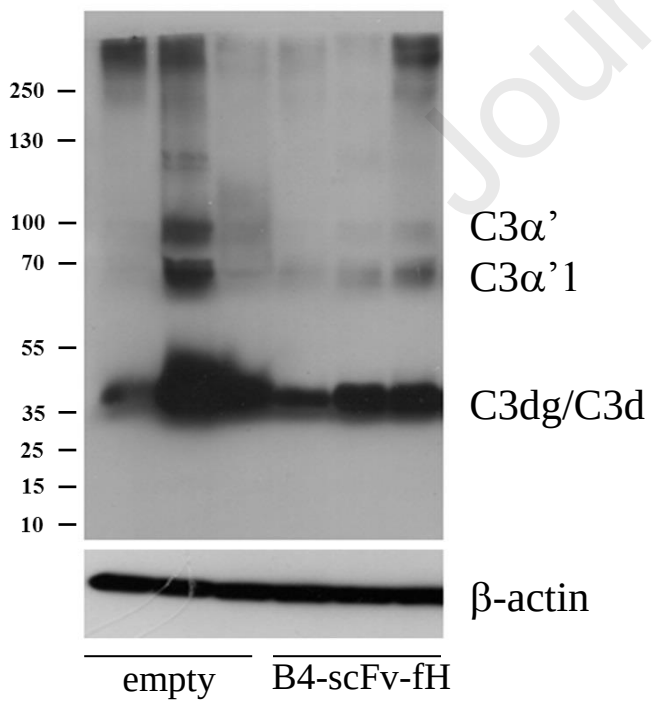

D'

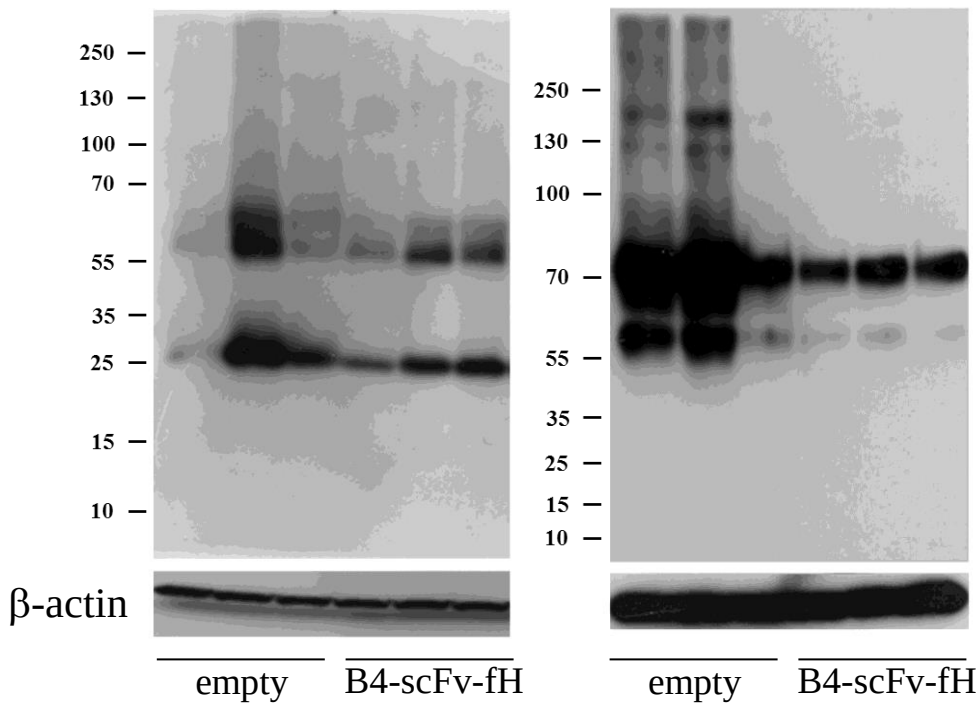

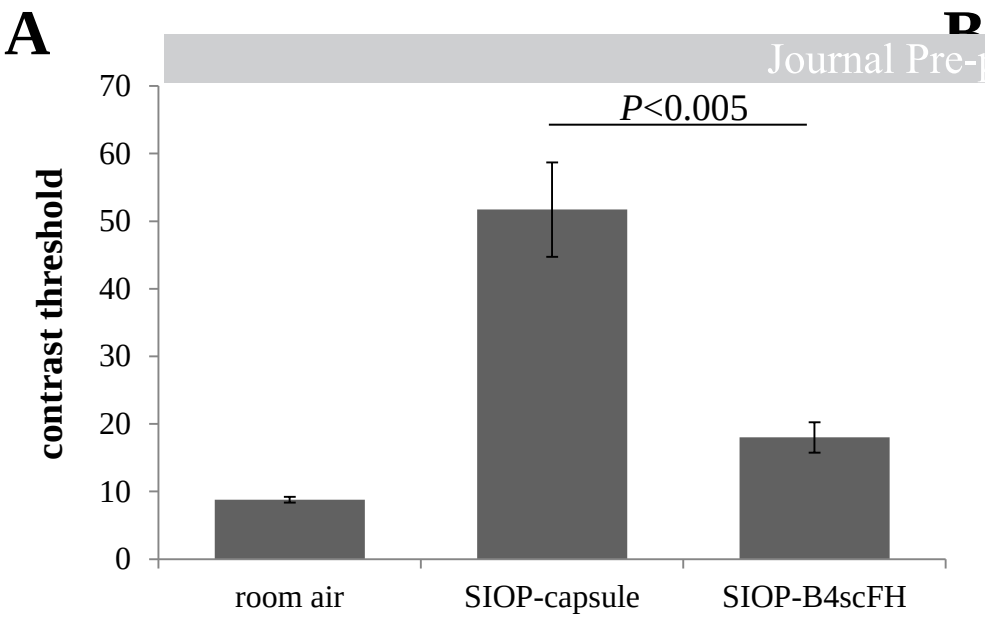

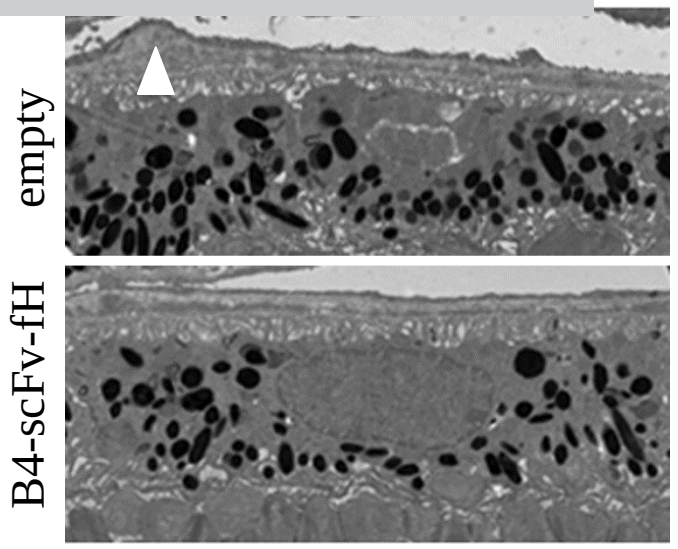

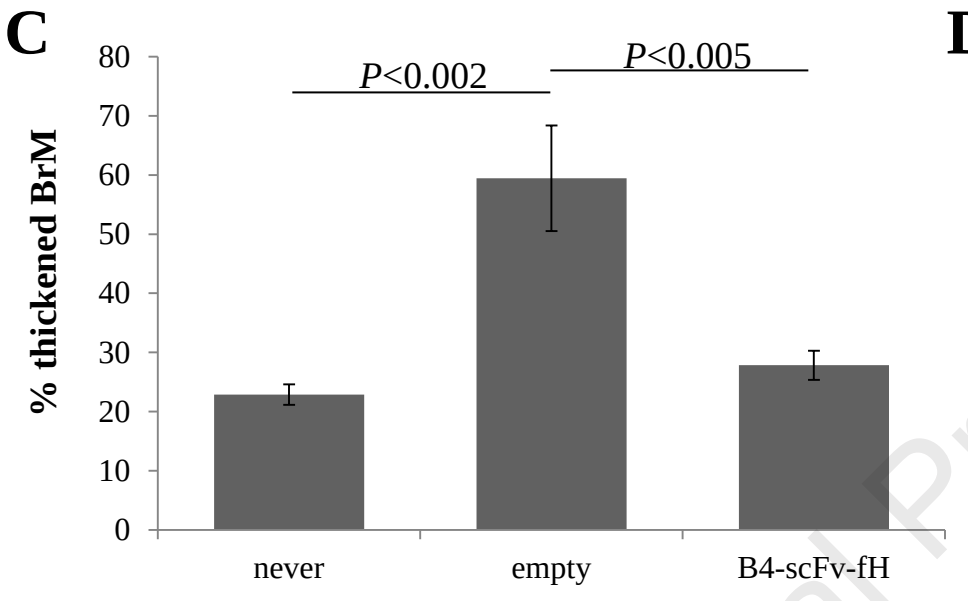

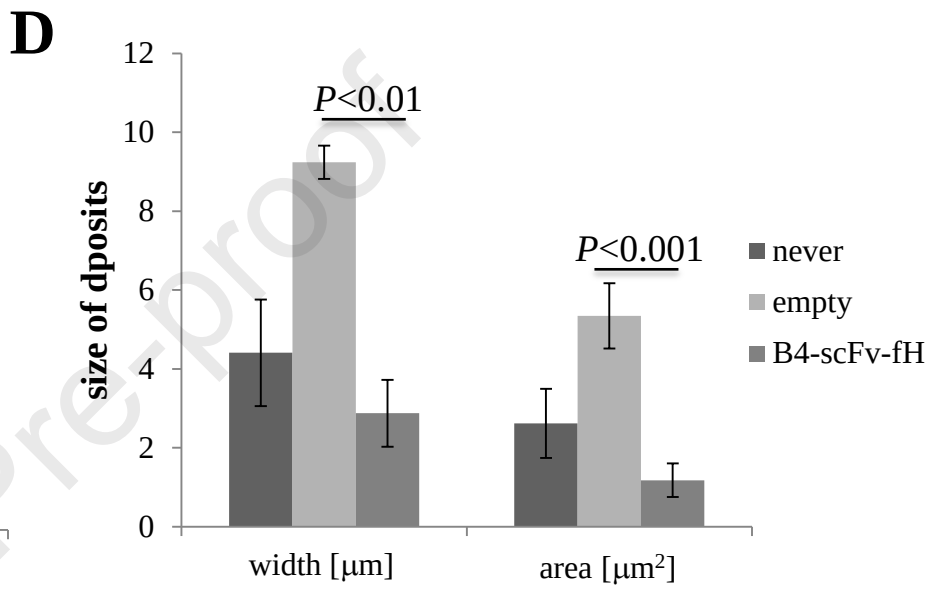

A

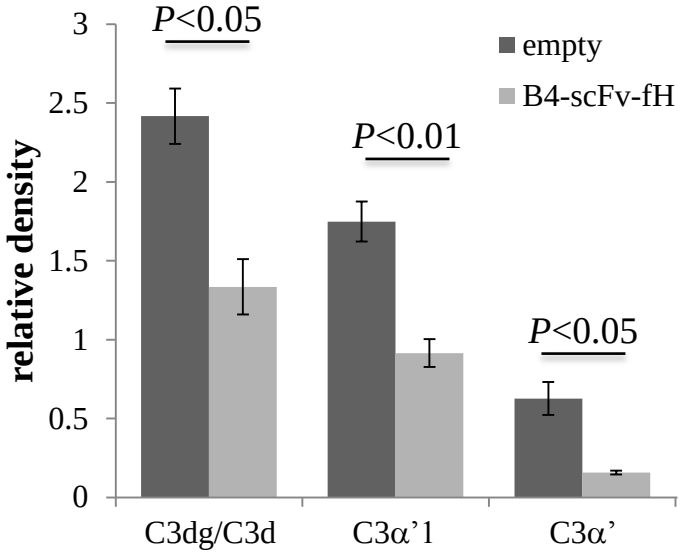

A' C3α breakdown products

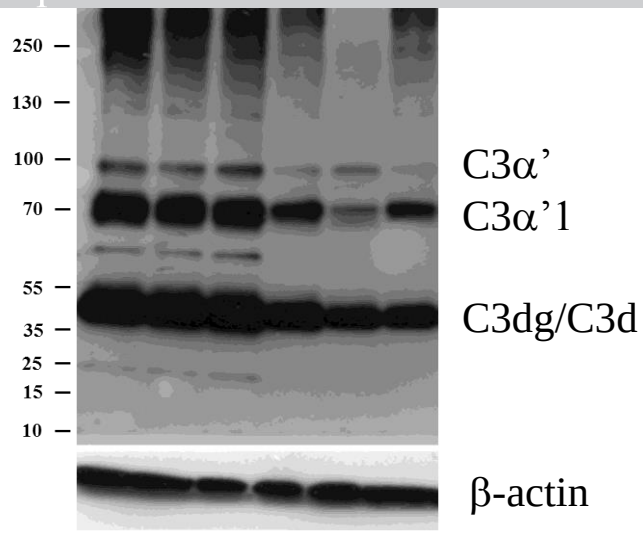

B

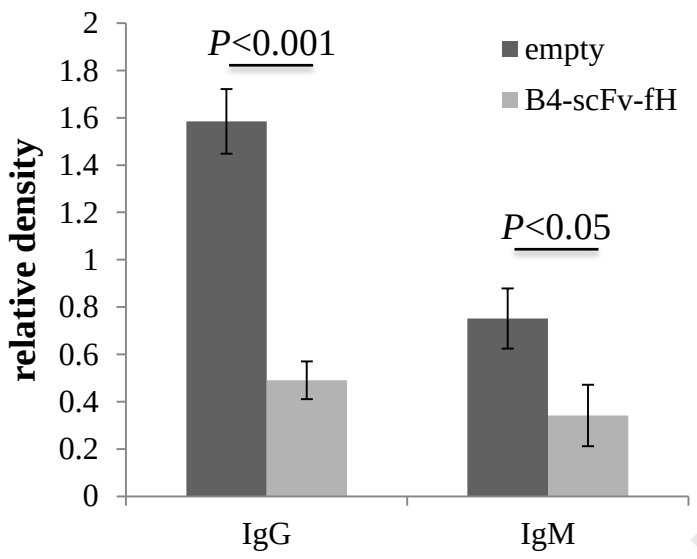

B'

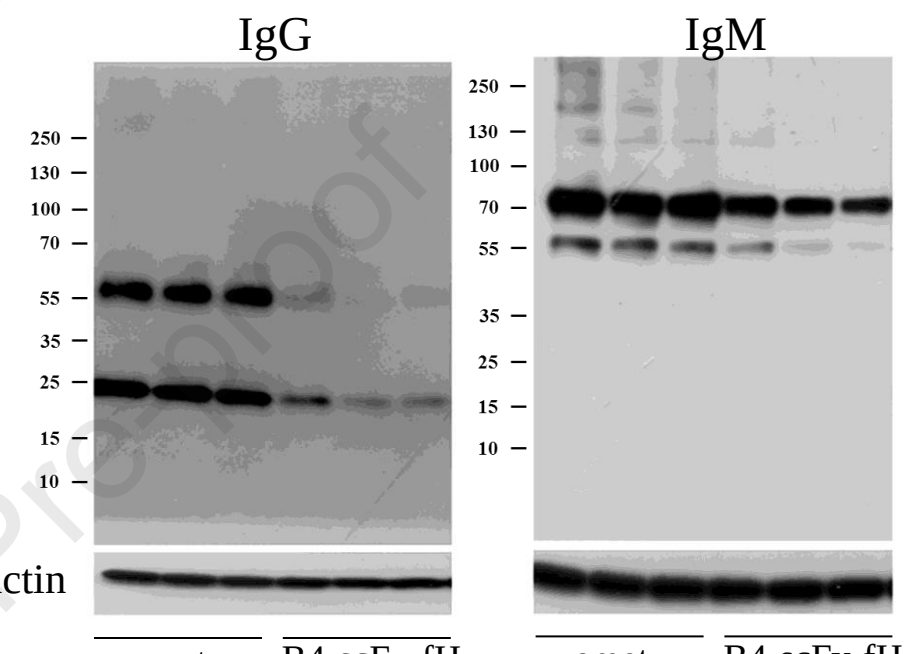

C

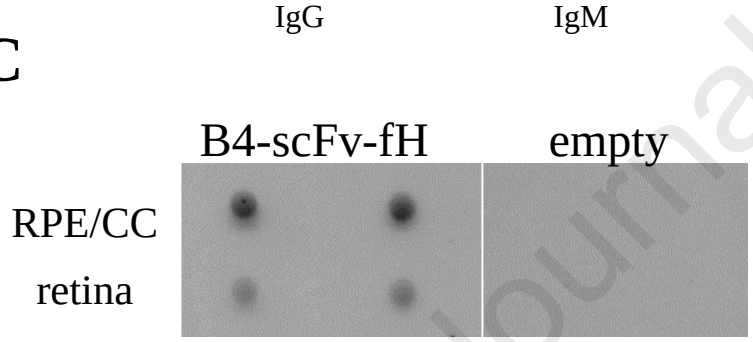

Precis: AMD risk is tied to an overactive complement system, and ocular injury is reduced by alternative pathway (AP) inhibition in experimental models. We developed a novel inhibitor of the AP that targets an injury-specific danger associated molecular pattern, and characterized it in disease models.